Non-linear boundary condition for non-ideal electrokinetic equations in porous media

Grégoire Allaire, Robert Brizzi, Christophe Labbez, Andro Mikelić

Non-linear boundary condition for non-ideal electrokinetic equations in porous media*

Grégoire Allaire, Robert Brizzi
E-mail: gregoire.allaire@polytechnique.fr; robert.brizzi@polytechnique.fr
CMAP, Ecole Polytechnique, Institut Polytechnique de Paris, F-91128 Palaiseau, France

Christophe Labbez
E-mail: christophe.labbez@u-bourgogne.fr
Université de Bourgogne Franche-Comté,
ICB UMR 6303 CNRS, Dijon, France

Andro Mikelić
Université Claude Bernard Lyon 1, CNRS UMR 5208,
Institut Camille Jordan
F-69622 Villeurbanne cedex, France

March 11, 2022

This collaborative work started in 2014 and was delayed for several years. In the spring of 2020 it was resumed but Andro Mikelic was struck by the illness that took him away in November 2020. His co-authors finished this manuscript and dedicate it to his memory.

Abstract

This paper studies the partial differential equation describing the charge distribution of an electrolyte in a porous medium. Realistic non-ideal effects are incorporated through the mean spherical approximation (MSA) model which takes into account finite size ions and screening effects. The main novelty is the consideration of a non-constant surface charge density on the pore walls. Indeed, a chemical equilibrium reaction is considered on the boundary to represent the dissociation of ionizable sites on the solid walls. The surface charge density is thus given as a non-linear function of the electrostatic potential. Even in the ideal case, the resulting system is a new variant of the famous Poisson-Boltzmann equation, which still has a monotone structure under quantitative assumptions on the physical parameters. In the non-ideal case, the MSA model brings in additional non-linearities which break down the monotone structure of the system. We prove existence, and sometimes uniqueness, of the solution. Some numerical experiments are performed in 2-d to compare this model with that for a constant surface charge.

pacs 02.30.Jr ; 47.57.J- ; 47.70.Fw ; 82.70.Dd ; 91.60.Pn . **keywords** Poisson-Boltzmann equation, MSA, electro-osmosis.

*This research was partially supported by the project MOMART from the program NEEDS (Projet fédérateur Milieux Poreux MIPOR) and the GdR MOMAS.

1 Introduction

This paper is devoted to the modeling, the mathematical analysis and some numerical experiments of the electrostatic properties of an electrolyte in a charged porous medium. In the so-called ideal case and when the surface charge of the solid porous medium is constant, this model is well-known in the literature under the name of Poisson-Boltzmann equation [13]. In the present work, we go beyond the ideal case by using the Mean Spherical Approximation (MSA) model, which considers ions to be charged hard spheres, takes into account their finite size and screening effects [4], [10]. This MSA model is known to improve the ideal model for high concentrations and small pores [3], [7]. We already studied this MSA model in our previous work [2]. Actually, the main novelty of the present paper is the analysis of a model of surface charge density, which is not any longer constant, but rather given as the output of a chemical equilibrium reaction on the pores boundaries which represents the dissociation of ionizable sites on the solid walls (see [5], [6], [12], [19] for a physico-chemical presentation). Note that the Poisson-Boltzmann equation and its variants are key ingredients to derive transport properties of electrolytes in porous media by means of homogenization or upscaling [1], [17], [18].

The precise model which is studied here is described in Section 2. For simplicity we start in Subsection 2.1 with the case of a salt free bulk solution, namely with H^+ as the single ion in the model. Indeed, the ionizable sites on the solid walls are of the type $M-OH$, where M is some metallic atom, and the dissociation reaction is $M-OH \leftrightarrow M-O^- + H^+$. In other words, only H^+ ions are involved in this chemical reaction at the boundary. For the sake of completeness, we recall in Subsection 2.2 the ideal model for this single H^+ ion. Finally, Subsection 2.3 describes our full model with several ions in the bulk. But still, only H^+ is involved in the non-linear boundary condition.

Section 3 is devoted to the mathematical analysis of this non-linear electrostatic model in the case of a single ion. For pedagogical reasons, the ideal model is first discussed before going to the MSA model. In the ideal case, the non-linearities of the partial differential equations are monotone, so the existence and uniqueness of a solution is easy, let apart the difficulty that the Poisson-Boltzmann equation involves an exponential non-linearity which is not integrable in full generality. Nevertheless, this kind of difficulty is classical in the literature (see [9], [14]): here we use a truncation argument and L^∞-bounds to prove existence of a solution. For the MSA model, we prove that the non-linearities are monotone under an assumption on the size of the ions (which must be not too small, see Proposition 13). Then, the existence proof for solutions is surprisingly simpler since the MSA model furnishes an upper bound on the ion concentration: Theorem 19 gives the existence and uniqueness of a solution, provided that a parameter δ, measuring the departure from the ideal case, is small enough.

Section 4 extends the mathematical analysis to the case of several ions. Again we begin with the easier ideal model before going to the more involved MSA model. In the ideal case, the non-linearities are again monotone and existence and uniqueness is easy, with the same arguments as in the case of a single ion (see Theorem 22). However, the MSA model is much more intricate. Although we can still prove that the bulk charge density is monotone under an assumption on the size of the ions (which must be not too small, see Proposition 29), we are unable to prove a similar result for the surface charge density. Fortunately, the MSA model still furnishes uniform upper bounds on the non-linearities, which allows us to prove existence of at least one solution (see Theorem 28).

Eventually Section 5 is concerned with some numerical experiments. In particular, comparisons are made between a constant surface charge density and the non-linear one which is proposed by our model of Section 2. Our conclusion is that, although the surface charge density may vary

significantly, the resulting potentials are quite similar.

2 Electrokinetic models

s.model

This work is restricted to equilibrium situations for an electrolyte in a charged rigid porous medium. In other words, the fluid containing the electrolyte is assumed to be at rest and only electrostatic equations are considered.

2.1 Single ion case

s.1ion

We first consider a simpler case with a salt free bulk solution (i.e. with a reservoir containing no ions). More precisely, only the counterions to the charge of the porous medium are considered. These counterions are H^+, implying that the surface of the solid porous medium is negatively charged as is the case in practice for rocks like clays.

As usual in porous media studies, we consider a representative volume element of a porous medium which, for simplicity, is a cube $Q = (0, L)^d$ with periodic boundary conditions ($d = 2, 3$ is the space dimension). The fluid part of Q is Ω_f and the solid part is Ω_s with $\Omega_f \cap \Omega_s = \emptyset$ and $\overline{Q} = \overline{\Omega_f} \cup \overline{\Omega_s}$. In the sequel, because of the finite size of ions, we shall rather consider another *effective* fluid domain $\Omega_D \subset \Omega_f$, which is slightly smaller than Ω_f and is the domain on which the equations are posed. Its internal boundary $\partial\Omega_D$ is the interface between the effective solid structure and the effective pore volume Ω_D. It is assumed to be smooth, say C^1. An example of Ω_D is shown on Figure 2.

The concentration of the sole type of ions, namely H^+, is denoted by n_H and its valence is $z_H = 1$. These H^+ ions come from the dissociation of ionizable sites, $M - OH$, located on the "hard" (non penetrating) surface of the solid porous medium, $\partial\Omega_s$. Here, M refers to some metallic atom. The dissociation reaction of $M - OH$ obeys the following chemical equilibrium

$$M - OH \leftrightarrow M - O^- + H^+, \tag{1}$$

chemreac

which gives rise to a surface charge distribution on $\partial\Omega_s$. The H^+ ions have a finite non-zero diameter σ_H. As a result they cannot lie on $\partial\Omega_s$ but rather stay at a distance not smaller than $\sigma_H/2$ from $\partial\Omega_s$. We, therefore, define another surface $\partial\Omega_D$ which is obtained from $\partial\Omega_s$ by a translation of $\sigma_H/2$ in the opposite normal direction. In other word, $\partial\Omega_D$ is the boundary of the Stern layer where the ion concentration starts to be non-zero. A generic point on $\partial\Omega_s$ is denoted by x_s and it is associated to a unique point x_D on $\partial\Omega_D$ (provided that the surface is smooth enough and σ_H is small enough, this point is uniquely defined by $x_D = x_s - (\sigma_H/2)n$ where n is the exterior unit normal). Note that the following equations (Poisson-Boltzmann and MSA model) are actually valid only up to $\partial\Omega_D$ because no ions can get closer to the hard surface $\partial\Omega_s$. In the sequel, Ω_D denotes the effective fluid part of the porous domain, enclosed by $\partial\Omega_D$.

The electrostatic potential is calculated from Poisson equation with the electric charge density as bulk source term

$$-\mathcal{E}\Delta\Psi = en_H \qquad \text{in} \quad \Omega_D, \tag{2}$$

AM3

where $\mathcal{E} > 0$ is the dielectric constant of the solvent and e is the (positive) electron charge. The boundary condition reads

$$\mathcal{E}\nabla\Psi \cdot \nu = -\Sigma^s \qquad \text{on} \quad \partial\Omega_D, \tag{3}$$

AM4

where ν is the unit exterior normal to the porous domain Ω_D and $-\Sigma^s$ denotes the surface charge density on $\partial\Omega_D$ which turns out to be equal to that on $\partial\Omega_s$, as we shall see in a few lines. We assume that the surface charge density on $\partial\Omega_s$ is negative, which translates as $\Sigma^s > 0$. The novelty of our model is that the value of Σ^s is not a data but is given as a non linear function of Ψ, as is detailed below.

For the moment, let us relate the ion concentration n_H to the potential Ψ. Let μ_H be the chemical potential of H^+ in the bulk given by

$$\mu_H = \mu_H^0 + k_B T \ln n_H + k_B T \ln \gamma_H, \tag{4}$$ Chempot

with γ_H being the *activity coefficient* of H^+, k_B the Boltzmann constant, μ_H^0 the standard chemical potential expressed at infinite dilution and T is the absolute temperature. All these quantities are constants in our model, except γ_H which depends on the concentration n_H. Indeed, as n_H increases, interactions between ions becomes non negligible and γ_H takes them into account. We model γ_H through the *Mean Spherical Approximation (MSA)* in simplified form [7]. The activity coefficient reads

$$\ln \gamma_H = -\frac{L_B \Gamma z_H^2}{1 + \Gamma \sigma_H} + \ln \gamma^{HS}, \tag{5}$$ gamma-j

where σ_H is the ion diameter of H^+, $z_H = 1$ is the valence of H^+, L_B is the Bjerrum length given by $L_B = e^2/(4\pi\mathcal{E}k_B T)$, γ^{HS} is the hard sphere term defined by (8) and Γ is the *MSA screening parameter* defined by

$$\Gamma^2 = \pi L_B \frac{n_H z_H^2}{(1 + \Gamma\sigma_H)^2}, \tag{6}$$ Gamma0

or equivalently by the positive root of (6)

$$\Gamma = \frac{2 z_H \sqrt{\pi L_B n_H}}{1 + \sqrt{1 + 4 z_H \sigma_H \sqrt{\pi L_B n_H}}}. \tag{7}$$ Gamma

In (5) the hard sphere term γ^{HS} is given by

$$\ln \gamma^{HS} = p(\xi) \equiv \xi \frac{8 - 9\xi + 3\xi^2}{(1-\xi)^3}, \quad \text{with} \quad \xi = \frac{\pi}{6} n_H \sigma_H^3, \tag{8}$$ Hardsphere

and ξ is called the solute packing fraction. From (5), (7) and (8) it is clear that γ_H is a function of n_H. Note that Γ in (7) is also a function of n_H.

The migration-diffusion flux $\mathbf{j}$ is given by the following linear relationship

$$\mathbf{j} = -L(n_H)\big(\nabla \mu_H + z_H e \nabla \Psi\big), \tag{9}$$ electroflux

where $L(n_H)$ is the (positive) Onsager coefficient. Under our equilibrium assumption, the migration-diffusion flux must vanish, $\mathbf{j} = 0$, which implies that $\mu_H + z_H e \Psi$ is constant, and, together with (4), leading to

$$n_H \gamma_H e^{\frac{z_H e \Psi}{k_B T}} = a_H, \tag{10}$$ equil

where a_H is a given positive constant, called the *activity* of H^+. This relation (10) gives n_H, the right hand side of (2), as a non-linear function of Ψ.

We now come to the modelling of the surface charge distribution on $\partial\Omega_s$, following classical works as [5], [6], [12], [19]. If a_{M-OH} and a_{M-O} denote the activities of $M-OH$ and $M-O^-$, respectively, the standard equilibrium constant $K^0 > 0$ for the dissociation reaction defined in (1) can be written as

$$K^0 = \frac{a_H a_{M-O}}{a_{M-OH}}.$$

Through a formula similar to (10) we compute the activities a_{M-OH} and a_{M-O} in terms of the surface concentrations n_{M-OH}, n_{M-O} and activity coefficients $\gamma_{M-OH}, \gamma_{M-O}$. More precisely, for any point on $\partial\Omega_s$ we have

$$a_{M-O} = \gamma_{M-O} n_{M-O} e^{\frac{z_{M-O} e\Psi}{k_B T}} \quad \text{and} \quad a_{M-OH} = \gamma_{M-OH} n_{M-OH} e^{\frac{z_{M-OH} e\Psi}{k_B T}}$$

with the valences $z_{M-OH} = 0$ and $z_{M-O} = -1$. Since $M-OH$ and $M-O^-$ are surface sites there are no hard sphere terms in the definitions of $\gamma_{M-OH}, \gamma_{M-O}$. Furthermore, since $M-OH$ is neutral, there is no screening effect for this type of site and we therefore assume $\gamma_{M-OH} = 1$, which implies that $a_{M-OH} = n_{M-OH}$. The surface charge density is simply

$$-\Sigma^s = e z_{M-O} n_{M-O} = -e n_{M-O} \tag{11}$$ Sigma1

since the valence is $z_{M-O} = -1$. The maximal possible charge is denoted by $\Sigma^s_{\max} > 0$. Since the number of ionizable sites is constant, equal to $n_{M-OH} + n_{M-O}$, the maximal possible charge is given by

$$e(n_{M-OH} + n_{M-O}) = \Sigma^s_{\max}.$$

We deduce

$$\Sigma^s = \frac{K^0 \Sigma^s_{\max}}{K^0 + \gamma_{M-O} \exp\{\frac{-e\Psi}{k_B T}\} a_H}. \tag{12}$$ Sigma4

To compute the activity coefficient γ_{M-O} we rely on a formula similar to (5). However there is a subtle point here: the screening parameter is due to H^+ ions which are not lying on the hard surface $\partial\Omega_s$ but are on the effective surface $\partial\Omega_D$. In other words, formula (12) holds for a point $x_s \in \partial\Omega_s$ but γ_{M-O} is evaluated at the corresponding point $x_D \in \partial\Omega_D$. Similarly, the potential $\Psi(x_s)$ on $\partial\Omega_s$ is different from the so-called diffuse potential or Stern potential $\Psi(x_D)$ on $\partial\Omega_D$. Formula (5) is adapted to this case by taking $\gamma^{HS} = 1$, since the surface concentration of H^+ is null on $\partial\Omega_s$, and $\sigma_H = 0$, since punctual surface sites are assumed, leading to the following formula for the activity coefficient of the charged sites, $M-O^-$,

$$\ln \gamma_{M-O} = -L_B z^2_{M-O} \Gamma(x_D) \tag{13}$$ gamma-D

where Γ is the surface screening parameter defined by (7).

Since there are no ions between the hard surface $\partial\Omega_s$ and the effective surface $\partial\Omega_D$, they form a capacitor with capacitance (for not too curved surfaces) defined as

$$C^s = 2\mathcal{E}/\sigma_H,$$

and the charge surface densities on $\partial\Omega_s$ and $\partial\Omega_D$ are equal, $\Sigma^s(x_s) = \Sigma^s(x_D)$, while the potential $\Psi(x_D)$ on $\partial\Omega_D$ is then related to $\Psi(x_s)$ on $\partial\Omega_s$ by

$$\Psi(x_s) = \Psi(x_D) - \Sigma^s / C^s.$$

From these last expressions we can substitute for γ_{M-O} and $\Psi(x_s)$ in (12) to get

$$\Sigma^s(x_D) = \frac{K^0 \Sigma^s_{\max}}{K^0 + a_H \exp\{-L_B z^2_{M-O} \Gamma(x_D)\} \exp\left\{\frac{-e}{k_B T}\left(\Psi(x_D) - \frac{\Sigma^s \sigma_H}{2\mathcal{E}}\right)\right\}}.$$

Defining

$$C_1 = \frac{e}{k_B T}, \quad C_2 = \frac{e\sigma_H}{2k_B T \mathcal{E}}, \quad C_3 = L_B,$$

(and recalling that K^0 and a_H are constant, independent of $x_D \in \partial\Omega_D$) we rewrite

$$\Sigma^s(x_D) = \frac{K^0 \Sigma^s_{\max}}{K^0 + a_H \exp\left\{-C_1 \Psi(x_D) + C_2 \Sigma^s(x_D) - C_3 \Gamma(x_D)\right\}},$$

which implicitly gives Σ^s as a non-linear function of Ψ on $\partial\Omega_D$. By some algebra and a logarithmic transformation, it is equivalent to

$$C_1 \Psi(x_D) = C_2 \Sigma^s(x_D) - C_3 \Gamma(x_D) - \ln\left(\frac{\Sigma^s_{\max}}{\Sigma^s(x_D)} - 1\right) - \ln \frac{K^0}{a_H}. \tag{14}$$

Sigma3

Eventually, our electrokinetic model is a combination of the Poisson-Boltzmann equation and MSA model in the bulk, and of a new non-linear boundary condition, issued from (14), which reads

$$\begin{cases} -\mathcal{E}\Delta\Psi = e n_H(\Psi) & \text{in} \quad \Omega_D, \\ \mathcal{E}\nabla\Psi \cdot \nu = -\Sigma^s(\Psi) & \text{on} \quad \partial\Omega_D, \\ x \mapsto \Psi(x) & \text{is } (0,L)^d\text{-periodic}, \end{cases} \tag{15}$$

Eqsinglequil1

where $n_H(\Psi)$ is a solution of the algebraic equation (10) and $\Sigma^s(\Psi)$ is a solution of the other algebraic equation (14).

The various physical parameters appearing in the above equations are defined in Table 1.

	QUANTITY	*CHARACTERISTIC VALUE*
e	electron charge	1.602e−19 C (Coulomb)
k_B	Boltzmann constant	1.38e−23 J/K
a_H	H^+ activity coefficient	$1.e-7$ mole/liter
T	temperature	$298°K$ (Kelvin)
$\mathcal{E}$	dielectric constant	6.9479e−10 $C/(mV)$
$\lambda_D = \sqrt{\frac{\mathcal{E}k_B T}{e^2 a_H}}$	Debye's length	1.3574 e−6 m
Σ^s_{max}	maximal surface charge density	$0.768 C/m^2$
σ_H	ionic hard sphere diameter	4e−10 m
$\zeta = k_B T/e$	characteristic electrokinetic potential	0.02567 V (Volt)
$L_B = e^2/(4\pi\mathcal{E}k_B T)$	Bjerrum length	7.14772e−10 m
K^0	dissociation reaction equilibrium constant	1.5849 e −10 mole/litre
$\Gamma_c = \sqrt{\pi L_B a_H}$	characteristic MSA screening parameter	0.3677 e6 1/m
$\xi_c = \frac{\pi}{6} a_H \sigma_H^3$	characteristic solute packing fraction	2.01 e −9
bi $= L_B/\sigma_H$	Bjerrum parameter	1.786

Table 1: *Data of the physical parameters* Data

sub22

2.2 Ideal model for a single H^+ ion

The MSA model introduces additional non-linearities, through the activity coefficient γ_H, in equation (15). In the dilute regime of small concentrations, the MSA model can be replaced by the simpler *ideal* model, which is easier to analyze. The present subsection is devoted to this simpler ideal case, which is defined by an activity coefficient $\gamma_H = 1$. Therefore, equation (10) simplifies

$$n_H^{id} = a_H e^{\frac{-z_H e\Psi}{k_B T}}. \tag{16}$$

equilideal

In the ideal case, the screening parameter Γ and the Bjerrum length are neglected, so the constant C_3 in (14) vanishes. The nonlinear equation (14) becomes

$$C_1\Psi(x_D) = C_2\Sigma_{id}^s(x_D) - \ln\left(\frac{\Sigma_{\max}^s}{\Sigma_{id}^s(x_D)} - 1\right) - \ln\frac{K^0}{a_H}. \tag{17}$$

Sigma3ideal

System (15) becomes

$$\begin{cases} -\mathcal{E}\Delta\Psi = en_H^{id}(\Psi) & \text{in} \quad \Omega_D, \\ \mathcal{E}\nabla\Psi\cdot\nu = -\Sigma_{id}^s(\Psi) & \text{on} \quad \partial\Omega_D, \\ x \mapsto \Psi(x) & \text{is } (0,L)^d\text{-periodic}, \end{cases} \tag{18}$$

Eqsinglequil2

which shall be analyzed in Subsection 3.1.

rem.limit

Remark 1. *The ideal model has been defined through a unit activity coefficient $\gamma_H = 1$. Actually, it is known to be the limit of the MSA model in the* dilute regime. *This limit was more precisely stated in lemma 1 of [2] introducing some characteristic parameters. Define the characteristic solute packing fraction parameter $\xi_c = \pi a_H \sigma_H^3/6$ and the Bjerrum parameter* bi $= \frac{L_B}{\sigma_H}$. *Then, the ideal case is the limit of the MSA model when $\xi_c \to 0$, while* bi *is fixed of order one.*

ss.model

2.3 Several ions case

We now consider a solution of N different ions in water, labelled by an index $i \in \{1, ..., N\}$. These ions are characterized by their valence z_i, diameter σ_i, concentration n_i and chemical potential μ_i. For the mathematical analysis of Subsection 4.2, we shall assume that all ions have the same diameter and that there are both positive and negative valences (which is always the case in practice when considering a salt like $Ca(OH)_2$). Of course, one of these ions is H^+ which is necessarily involved in the dissociation reaction of ionizable sites on the pore surface. The Poisson equation (2) is changed to

$$-\mathcal{E}\Delta\Psi = e\sum_{i=1}^{N} z_i n_i \qquad \text{in} \quad \Omega_D. \tag{19}$$

3.AM3

The chemical potential μ_i is given by

$$\mu_i = \mu_i^0 + k_B T \ln n_i + k_B T \ln \gamma_i, \tag{20}$$

3.Chempot

where γ_i is the activity coefficient of ion i which, according to the MSA model, is defined by

$$\ln\gamma_i = -\frac{L_B\Gamma z_i^2}{1+\Gamma\sigma_i} + \ln\gamma^{HS}, \tag{21}$$

3.gamma-j

where Γ is the MSA screening parameter defined by

$$\Gamma^2 = \pi L_B \sum_{i=1}^{N} \frac{n_i z_i^2}{(1+\Gamma\sigma_i)^2}, \tag{22}$$ 3.Gamma

and γ^{HS} is the hard sphere term given by

$$\ln \gamma^{HS} = p(\xi) \equiv \xi \frac{8-9\xi+3\xi^2}{(1-\xi)^3}, \quad \text{with} \quad \xi = \frac{\pi}{6}\sum_{i=1}^{N} n_i \sigma_i^3, \tag{23}$$ 3.Hardsphere

where ξ is the solute packing fraction.

The migration-diffusion flux $\mathbf{j}_i$ of ion i is given by the following linear relationship

$$\mathbf{j}_i = -\sum_{j=1}^{N} L_{ij}\big(\nabla\mu_j + z_j e \nabla\Psi\big), \quad i = 1, \dots, N, \tag{24}$$ 3.electroflux

where L_{ij} is the Onsager coefficient (the Onsager tensor is assumed to be positive definite, thus invertible). At equilibrium, all migration-diffusion fluxes must vanish, $\mathbf{j}_i = 0$, a condition which is satisfied if $\mu_j + z_j e\Psi$ is constant for all $j = 1, \dots, N$, or equivalently

$$n_j \gamma_j e^{\frac{z_j e \Psi}{k_B T}} = a_j, \quad j = 1, \dots, N, \tag{25}$$ 3.equil

where a_j is a given positive constant defining the *activity* of ion j. The collection of relations (25), together with (21), (22) and (23), gives all n_i, in the right hand side of (19), as a non-linear function of Ψ.

The Neumann boundary condition (3), as well as the modelling of the surface charge distribution Σ^s on the boundary $\partial\Omega_D$, are the same as in the case of a single ion since it involves only the surface sites $M-OH$ and $M-O^-$, together with the H^+ ion. In particular, formulas (12) and (13) still hold true. However, the surface screening parameter $\Gamma(x_D)$ should be evaluated with formula (22) instead of the previous one (6). The rest of the derivation is the same and the previous nonlinear Neumann boundary condition is still valid.

Eventually, the electrokinetic model is a combination of the Poisson-Boltzmann equation, of the MSA model in the bulk, and of the non-linear boundary condition, issued from (14), which reads

$$\begin{cases} -\mathcal{E}\Delta\Psi = e\displaystyle\sum_{i=1}^{N} z_i n_i(\Psi) & \text{in} \quad \Omega_D, \\ \mathcal{E}\nabla\Psi\cdot\nu = -\Sigma^s(\Psi) & \text{on} \quad \partial\Omega_D, \\ x \mapsto \Psi(x) & \text{is } (0,L)^d\text{-periodic}, \end{cases} \tag{26}$$ Eqmulti

where $n_i(\Psi)$ is a solution of the system of algebraic equations (25), (21), (22) and (23), while $\Sigma^s(\Psi)$ is a solution of the other algebraic equation (14).

rem.valence **Remark 2.** *The periodic boundary condition in* (26) *implies a global electroneutrality condition, namely*

$$e\int_{\Omega_D}\sum_{i=1}^{N} z_i n_i(\Psi)\,dx = \int_{\partial\Omega_D}\Sigma^s(\Psi)\,dx.$$

In other words, the surface charge on $\partial\Omega_D$ is exactly compensated by the bulk charge in Ω_D, due to the ion densities. The same would be true with homogeneous Neumann boundary condition on the exterior boundary of the cube $(0,L)^d$. Since, by definition, $0 \le \Sigma^s \le \Sigma^s_{\max}$, it implies that all valences z_i cannot be negative and there must be at least one which is positive (recall that the valences z_i are non-zero relative integers). Indeed, as already said, the ion H^+ with $z_{H^+} = 1$ is always in the list of ions since it appears in the dissociation reaction of ionizable sites on the pore surface. In most practical cases, the solution contains both anions and cations, that is positive and negative values of the valences z_i.

3 Mathematical analysis in the single ion case

s.analysis

This section is concerned with the existence of solutions for the nonlinear boundary value problem (15). The fact that periodic boundary conditions are enforced on the cubic domain $(0,L)^d$ is irrelevant and other outer boundary conditions (like Dirichlet or Neumann) do not change our results. To simplify the notations, and thus the analysis, we first re-write the equations in their dimensionless form.

3.1 Ideal model

ss.ideal

The ideal case of Subsection 2.2 is much simpler, so we start with its analysis. In particular, equation (18) is the Euler-Lagrange condition for the minimization of a convex energy (see Remark 4), which makes its analysis especially easy.

To write dimensionless equations, we introduce dimensionless quantities τ and τ_B, defined by

$$\tau = ea_H L^2/(\zeta\mathcal{E}), \quad \tau_B = \Sigma^s_{max} L/(\zeta\mathcal{E}), \tag{27}$$

def.tau

where $\zeta = k_B T/e$ is the characteristic electrokinetic potential. A scaled space variable is also introduced as $x = L\tilde{x}$, with domain $\Omega_D = L\tilde{\Omega}_D$. The dimensionless unknowns are denoted with a tilde :

$$n^{id}_H(x) = a_H \tilde{n}^{id}_H(\tilde{x}), \quad \Psi(x) = \zeta\tilde{\Psi}(\tilde{x}) \quad \text{and} \quad \Sigma^s_{id}(x) = \Sigma^s_{max}\tilde{\Sigma}^s_{id}(\tilde{x}).$$

Then, equation (16) simplifies

$$\tilde{n}^{id}_H = e^{-\tilde{\Psi}}$$

and, similarly, the nonlinear equation (17) becomes

$$\tilde{\Psi} = C_2\Sigma^s_{max}\tilde{\Sigma}^s_{id} - \ln\left(\frac{1}{\tilde{\Sigma}^s_{id}} - 1\right) - \ln\frac{K^0}{a_H}. \tag{28}$$

Sigma3ideal2

For simplicity, in the sequel we skip the tilde notation. System (18) now reads

$$\begin{cases} -\Delta\Psi = \tau e^{-\Psi} & \text{in} \quad \Omega_D, \\ \nabla\Psi\cdot\nu = -\tau_B\Sigma^s_{id}(\Psi) & \text{on} \quad \partial\Omega_D, \\ x \mapsto \Psi(x) & \text{is } (0,1)^d\text{-periodic}, \end{cases} \tag{29}$$

Eqsinglequilid1

where $\Sigma^s_{id}(\Psi)$ is uniquely defined by (28) as shown in the next lemma.

lem.sigmas

Lemma 3. *For any value of Ψ, there exists a unique solution $\Sigma^s_{id}(\Psi)$ of equation (28) and the function $\Psi \mapsto \Sigma^s_{id}(\Psi)$ is strictly monotone increasing from $\mathbb{R}$ into $(0,1)$.*

Proof. Formula (28) yields

$$\frac{d\Psi}{d\Sigma_{id}^s} = C_2\Sigma_{\max}^s + \frac{1}{\Sigma_{id}^s(1-\Sigma_{id}^s)} > 0 \quad \text{for} \quad 0 < \Sigma_{id}^s < 1.$$

Hence Σ_{id}^s is a strictly monotone increasing function of Ψ. □

We introduce the Sobolev space $H^1_{\#}(\Omega_D)$, defined by

$$H^1_{\#}(\Omega_D) = \{\phi \in H^1(\Omega_D) \mid \phi \text{ is } (0,1)^d\text{-periodic }\}.$$

A variational formulation of problem (29) is: find $\Psi \in H^1_{\#}(\Omega_D) \cap L^\infty(\Omega_D)$ such that

$$\int_{\Omega_D} \nabla\Psi \cdot \nabla\phi \, dx - \tau \int_{\Omega_D} e^{-\Psi}\phi \, dx + \tau_B \int_{\partial\Omega_D} \Sigma_{id}^s(\Psi)\phi \, ds = 0, \quad \forall \phi \in H^1_{\#}(\Omega_D). \tag{30}$$ Varforid

Note that the solution Ψ is required to belong to $L^\infty(\Omega_D)$ so that the exponential non-linearity is well defined. On the contrary, the boundary nonlinearity $\Sigma_{id}^s(\Psi)$ does not require $\Psi \in L^\infty(\Omega_D)$ since it is a bounded function by Lemma 3.

rem.convex **Remark 4.** *Solving the boundary value problem (29) or the variational formulation* (30) *is formally equivalent to minimizing the following energy*

$$E(\psi) = \frac{1}{2}\int_{\Omega_D} |\nabla\psi|^2 dx + \tau \int_{\Omega_D} e^{-\psi} dx + \tau_B \int_{\partial\Omega_D} \Xi_{id}^s(\psi) ds,$$

where $\Xi_{id}^s(\psi)$ is a primitive of $\Sigma_{id}^s(\psi)$. Since $\Sigma_{id}^s(\psi)$ is strictly monotone increasing, its primitive $\Xi_{id}^s(\psi)$ is convex. Therefore the energy $E(\psi)$ is strictly convex. Existence and uniqueness of a minimizer would be very easy if there were not the problem that the exponential term $e^{-\psi}$ is not well defined in the natural energy space $H^1_{\#}(\Omega_D)$ as soon as the space dimension d is larger than 1. Our remedy is to truncate the exponential non-linearity, prove uniform $L^\infty(\Omega_D)$ bounds and take the limit when the truncation parameter tends to infinity.

Trueexistid **Theorem 5.** *The variational formulation (30) has a unique solution in $H^1_{\#}(\Omega_D) \cap L^\infty(\Omega_D)$.*

To prove Theorem 5 requires some auxiliary results.

Definition 6. *For $M \in \mathbb{R}$, a cut-off function of $n_H^{id}(\phi) = e^{-\phi}$ is defined by*

$$n_M(\phi) = \begin{cases} e^{-\phi}, & \text{for } \phi \geq -M, \\ e^{M}, & \text{for } \phi < -M. \end{cases} \tag{31}$$ nhcutoffid

In particular, this cut-off function is bounded, $0 < n_M(\phi) \leq e^M$ for any $\phi \in \mathbb{R}$.

Introduce the cut-off version of the variational formulation (30): find $\Psi_M \in H^1_{\#}(\Omega_D)$ such that

$$\int_{\Omega_D} \nabla\Psi_M \cdot \nabla\phi \, dx - \tau \int_{\Omega_D} n_M(\Psi_M)\phi \, dx + \tau_B \int_{\partial\Omega_D} \Sigma_{id}^s(\Psi_M)\phi \, ds = 0, \quad \forall \phi \in H^1_{\#}(\Omega_D). \tag{32}$$ Varforiddelta

Next we introduce an auxiliary Neumann problem

$$\begin{cases} -\Delta U = \dfrac{|\partial\Omega_D|}{|\Omega_D|} & \text{in} \quad \Omega_D, \\ \nabla U \cdot \nu = -1 & \text{on} \quad \partial\Omega_D, \\ x \mapsto U(x) & \text{is } (0,1)^d\text{-periodic}, \end{cases} \tag{33}$$ Auxeq1

which has a unique solution $U \in H^1_{\#}(\Omega_D)/\mathbb{R}$, i.e. up to an additive constant (the choice of which does not influence our results, as we shall see). Furthermore, since the boundary of Ω_D is smooth, so is the solution and $U \in C(\overline{\Omega}_D)$.

Lemma 7. *Define*

$$\underline{\Psi}(x) = \tau_B \left(U(x) - \max_{\overline{\Omega}_D} U \right) + \ln \left(\frac{|\Omega_D|\tau}{|\partial\Omega_D|\tau_B} \right), \tag{34}$$ subPsi

and

$$\overline{\Psi}(x) = \frac{\tau_B}{2} \left(U(x) - \min_{\overline{\Omega}_D} U \right) + \max \left((\Sigma^s_{id})^{-1}(\frac{1}{2}), \ln \frac{2|\Omega_D|\tau}{|\partial\Omega_D|\tau_B} \right). \tag{35}$$ superPsi

Then, $\underline{\Psi}$ is a subsolution and $\overline{\Psi}$ is a supersolution for problem (32) when $M \geq -\min_{\overline{\Omega}_D} \underline{\Psi}$.

Proof. Take $M \geq -\min_{\overline{\Omega}_D} \underline{\Psi}$, so that $n_M(\underline{\Psi}) = e^{-\underline{\Psi}}$. Using the variational formulation of (33) for U, a direct calculation gives for any $\phi \geq 0,\ \phi \in H^1_{\#}(\Omega_D)$

$$\int_{\Omega_D} \nabla\underline{\Psi} \cdot \nabla\phi \, dx - \tau \int_{\Omega_D} n_M(\underline{\Psi})\phi \, dx + \tau_B \int_{\partial\Omega_D} \Sigma^s_{id}(\underline{\Psi})\phi \, ds =$$

$$\tau_B \int_{\partial\Omega_D} \big(\Sigma^s_{id}(\underline{\Psi}) - 1\big)\phi \, ds + \frac{|\partial\Omega_D|\tau_B}{|\Omega_D|} \int_{\Omega_D} (1 - \exp\{-\tau_B(U - \max_{\overline{\Omega}_D} U)\})\phi \, dx \leq 0. \tag{36}$$ subcal1

Hence $\underline{\Psi}$ is a subsolution for problem (32). A similar calculation gives for any $\phi \geq 0,\ \phi \in H^1_{\#}(\Omega_D)$

$$\int_{\Omega_D} \nabla\overline{\Psi} \cdot \nabla\phi \, dx - \tau \int_{\Omega_D} n_M(\overline{\Psi})\phi \, dx + \tau_B \int_{\partial\Omega_D} \Sigma^s_{id}(\overline{\Psi})\phi \, ds \geq$$

$$\tau_B \int_{\partial\Omega_D} \big(\Sigma^s_{id}(\overline{\Psi}) - \frac{1}{2}\big)\phi \, ds + \frac{|\partial\Omega_D|\tau_B}{2|\Omega_D|} \int_{\Omega_D} (1 - \exp\{-\frac{\tau_B}{2}(U - \min_{\overline{\Omega}_D} U)\})\phi \, dx \geq 0, \tag{37}$$ superX

where we additionally used the strict monotonicity of Σ^s_{id} and the fact that $\overline{\Psi}(x) \geq (\Sigma^s_{id})^{-1}(\frac{1}{2})$. Hence $\overline{\Psi}$ is a supersolution for problem (32). □

Having found a subsolution and a supersolution, we are in a position to apply Perron's method to establish the existence of a solution for problem (32). This is a very classical process and the interested reader is referred to the textbook [8] (section 9.3) and to the monograph [15] for more details and references.

tsingleideal **Proposition 8.** *There exists a weak solution of problem (32), $\Psi_M \in H^1_{\#}(\Omega_D) \cap L^\infty(\Omega_D)$, such that*

$$\underline{\Psi} \leq \Psi_M \leq \overline{\Psi} \quad a.e.\ in \quad \Omega_D.$$

We skip the proof of Proposition 8 which can be found, for example, in [8], pages 544-546.

Proof of Theorem 5. Choosing $M \geq -\min_{\overline{\Omega}_D} \underline{\Psi}$ we have $\Psi_M \geq \underline{\Psi}$ and $n_M(\Psi_M) = e^{-\Psi_M}$. Thus Ψ_M is also a solution of problem (30). The uniqueness of the solution $\Psi = \Psi_M$ is easily deduced from the monotonicity of the nonlinearities. □

3.2 MSA model

sub21bis

3.2.1 Adimensionalization and scaling of the MSA parameters

Here again we write the equations with dimensionless unknowns. To do so we introduce characteristic values of the physical parameters which are denoted with a subscript c. As before a_H is the characteristic ion concentration. We define a characteristic MSA screening parameter Γ_c and a characteristic solute packing fraction parameter ξ_c by

$$\Gamma_c = \sqrt{\pi L_B a_H} \quad \text{and} \quad \xi_c = \pi a_H \sigma_H^3/6. \tag{38}$$

coeff1

Introducing the Bjerrum parameter

$$\mathrm{bi} = \frac{L_B}{\sigma_H}, \tag{39}$$

coeff2

we define two coefficients

$$\alpha = \frac{\Gamma_c L_B}{\sqrt{\xi_c}} = \sqrt{6}\mathrm{bi}^{3/2} \quad \text{and} \quad \beta = \frac{\Gamma_c \sigma_H}{\sqrt{\xi_c}} = \sqrt{6}\mathrm{bi}^{1/2}. \tag{40}$$

coeff3

According to [2] (see Remark 1), the ideal case is the limit of the MSA model when $\xi_c \to 0$, while bi is fixed of order one. Therefore, in the sequel we shall assume some precise bounds on bi in order to analyze the non-linearities of the MSA model. Since bi is assumed to be of order one, so are α, β and thus

$$\Gamma_c \sigma_H = O(\sqrt{\xi_c}) \quad \text{and} \quad \Gamma_c L_B = O(\sqrt{\xi_c}). \tag{41}$$

coeffgamma

Based on this scaling we define a small parameter δ by

$$\delta = \sqrt{\xi_c}.$$

Recalling the scaled space variable $\tilde{x} = x/L$, we introduce dimensionless unknowns, denoted with a tilde,

$$n_H(x) = a_H \tilde{n}_H(\tilde{x}), \quad \Psi(x) = \zeta\tilde{\Psi}(\tilde{x}), \quad \Gamma(x) = \Gamma_c\tilde{\Gamma}(\tilde{x}), \quad \xi(x) = \delta^2\tilde{\xi}(\tilde{x}), \quad \Sigma^s(x) = \Sigma^s_{max}\tilde{\Sigma}^s(\tilde{x}),$$

where we recall that $\zeta = k_B T/e$. For readability we skip the tildes in the sequel.

Since $z_H = 1$, the non-linear algebraic equations (7), (10) and (14) become in adimensionalized form

$$\Gamma = \frac{2\sqrt{n_H}}{1 + \sqrt{1 + 4\beta\delta\sqrt{n_H}}}, \tag{42}$$

rootGamma

$$\ln n_H + \Psi - \delta\frac{\alpha\Gamma}{1 + \beta\delta\Gamma} + p(\delta^2 n_H) = 0, \tag{43}$$

logequil

$$\Psi = \frac{\sigma_H \Sigma^s_{max}}{2\mathcal{E}\zeta}\Sigma^s - \alpha\delta\Gamma - \ln(\frac{1}{\Sigma^s} - 1) - \ln\frac{K^0}{a_H}, \tag{44}$$

dsSigma

where the function $p(\xi)$ is defined by (8) for the hard sphere term. Similarly the adimensional form of system (15) is

$$\begin{cases} -\Delta\Psi = \tau n_H(\Psi) & \text{in} \quad \Omega_D, \\ \nabla\Psi\cdot\nu = -\tau_B\Sigma^s(\Psi) & \text{on} \quad \partial\Omega_D, \\ x \mapsto \Psi(x) & \text{is } (0,1)^d\text{-periodic}, \end{cases} \tag{45}$$

Eqsinglequilid3

where the positive parameters τ and τ_B are defined by (27). In the next subsection we check (under some technical conditions) that (42) and (43) unambiguously define $n_H(\Psi)$ and that $\Sigma^s(\Psi)$ is uniquely defined by (44).

3.2.2 Monotony properties of the functions $n_H(\Psi)$ and $\Sigma^s(\Psi)$

sub21

We first study the variations of Γ as a function of n_H.

propGamma

Lemma 9. *The MSA screening parameter Γ, defined by (42), is a smooth strictly monotone increasing function of $n_H \in (0, +\infty)$.*

Proof. Obviously, $\Gamma(n_H)$ is an infinitely smooth function for $n_H > 0$. A simple computation yields

$$\frac{d\Gamma}{d\sqrt{n_H}} = \frac{1}{1 + 2\beta\delta\Gamma} > 0,$$

thus Γ is a strictly monotone increasing function of n_H. □

Next we study the variations of n_H as a function of Ψ. From formulae (43) and (42), it is clear that $n_H \mapsto \Psi(n_H)$ is a well defined function on $(0, 1/\delta^2)$. However, it is its inverse function which is required as the right hand side in the Poisson equation (45).

monotonnH

Lemma 10. *Assume the Bjerrum parameter* $\mathrm{bi} = L_B/\sigma_H$ *satisfies the upper bound* $\mathrm{bi} \leq 6 + 4\sqrt{2}$. *Then, $\Psi \mapsto n_H(\Psi)$ is a strictly monotone decreasing function from $\mathbb{R}$ into $(0, 1/\delta^2)$ (and thus one-to-one).*

Proof. Replacing Γ in (43) by its formula (42) yields an explicit formula for Ψ as a function of $n_H \in (0, 1/\delta^2)$ (the solute packing fraction $\xi = \delta^2 n_H$ must stay in the range $(0, 1)$). It is easy to see that the limits of $\Psi(n_H)$ when n_H goes to 0, resp. to $1/\delta^2$, is $+\infty$, resp. $-\infty$. So the range of $\Psi(n_H)$ is $\mathbb{R}$. Differentiating (43) leads to

$$\frac{d\Psi(n_H)}{dn_H} = -\frac{1}{n_H} + \frac{\alpha\delta}{(1 + \beta\delta\Gamma)^2}\frac{d\Gamma(n_H)}{dn_H} - \delta^2 p'(\delta^2 n_H), \tag{46}$$

logequilsansdPsi2

$$\frac{d\Gamma(n_H)}{dn_H} = \frac{1}{2\sqrt{n_H}(1 + 2\beta\delta\Gamma)}. \tag{47}$$

logequilsansdPsi3

We insert expression (47) for the derivative of Γ into (46). The derivative of the hard sphere term $p(\xi)$, given by formula (8), is positive

$$p'(\xi) = 2\frac{4 - \xi}{(1 - \xi)^4} > 0 \quad \text{for } 0 \leq \xi < 1.$$

Hence to prove $\dfrac{d\Psi(n_H)}{dn_H} < 0$, it is sufficient to show that

$$0 \geq -\frac{1}{n_H} + \frac{\alpha\delta}{2\sqrt{n_H}}\frac{1}{(1 + 2\beta\delta\Gamma)(1 + \beta\delta\Gamma)^2} = \frac{-4(\beta\delta\Gamma)^2 + (\alpha/\beta - 6)\beta\delta\Gamma - 2}{2n_H(1 + 2\beta\delta\Gamma)(1 + \beta\delta\Gamma)} \tag{48}$$

formula2.nh

where we used

$$\sqrt{n_H} = \Gamma(1 + \sqrt{6\mathrm{bi}}\delta\Gamma). \tag{49}$$

formula.nh

Recall that $\alpha/\beta = \mathrm{bi}$. The numerator in the last expression of the right hand side of (48) is a polynomial of degree 2 in the variable $\beta\delta\Gamma$ and its discriminant is equal to $(\mathrm{bi} - 6)^2 - 32$. For $6 - 4\sqrt{2} < \mathrm{bi} < 6 + 4\sqrt{2}$, this discriminant is negative, therefore the polynomial has no real roots and is always negative. Furthermore, for $\mathrm{bi} \leq 6 - 4\sqrt{2}$ the roots of this polynomial are strictly negative and for positive Γ the expression remains strictly negative. Therefore, the condition $\mathrm{bi} \leq 6 + 4\sqrt{2}$ is sufficient for the decreasing character of $\Psi(n_H)$, which is thus invertible on its range. □

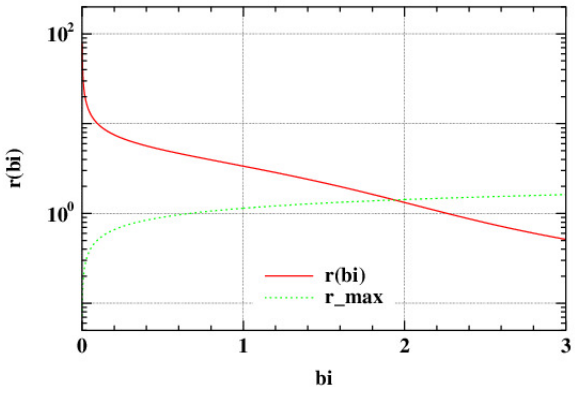

Figure 1: Variations of $r(\mathrm{bi})$ and $r_{max}(\mathrm{bi})$ as functions of the Bjerrum parameter bi. fig.rbi

PBcomment1 **Remark 11.** *From the data of Table 1 we find that* $\mathrm{bi} \approx 1.786 < 6 + 4\sqrt{2}$, *so the assumption of Lemma 10 is satisfied. Furthermore, under this assumption the bulk source nonlinearity in the Poisson-Boltzmann equation* (45) *derives from a convex energy (cf. Remark 4). The invertibility of the function* $\Psi(n_H)$ *can be guaranteed under less stringent conditions, but not its monotone character (see [2] for more details).*

rem.Gamma **Remark 12.** *By combining Lemmata 9 and 10, it is immediate that* $\Psi \mapsto \Gamma(\Psi)$ *is a decreasing function from* $\mathbb{R}$ *into its range* $(0, \Gamma_{max})$ *with the maximal value, corresponding to* $n_H = 1/\delta^2$,

$$\Gamma_{max} = \frac{r_{max}(\mathrm{bi})}{\beta\delta} \quad \text{with } r_{max}(\mathrm{bi}) = \frac{2\beta}{1+\sqrt{1+4\beta}} \quad \text{and } \beta = \sqrt{6\mathrm{bi}}. \tag{50}$$ gammamax

Eventually, we now prove that the surface charge density Σ^s is well defined by (44) and is an increasing function of the potential Ψ.

bdrynonlin **Proposition 13.** *Assume that* $\mathrm{bi} \le 3$. *Define a polynomial of degree 3*

$$P_3(w) = \mathrm{bi}w^3 + 2\mathrm{bi}(\mathrm{bi}-2)w^2 + (2\mathrm{bi}-6)w - 2. \tag{51}$$ P3

Then P_3 *admits a unique positive root* $r(\mathrm{bi})$. *Define*

$$\Psi_s = \begin{cases} 2\ln\delta + C_0 & \text{if } r(\mathrm{bi}) \le r_{max}(\mathrm{bi}), \\ -\infty & \text{if } r(\mathrm{bi}) > r_{max}(\mathrm{bi}), \end{cases} \tag{52}$$ psis

with a constant C_0, *independent of* $\delta > 0$, *given by*

$$C_0 = 2\ln\frac{\sqrt{6\mathrm{bi}}}{r(\mathrm{bi})(1+r(\mathrm{bi}))} + \frac{\mathrm{bi}\,r(\mathrm{bi})}{1+r(\mathrm{bi})} - p\left(\frac{r(\mathrm{bi})^2(1+r(\mathrm{bi}))^2}{6\mathrm{bi}}\right).$$

The algebraic equations (42), (43) *and (44) uniquely define a function* $\Psi \mapsto \Sigma^s(\Psi)$ *which is strictly monotone increasing from* $(\Psi_s, +\infty)$ *into its range* $(\Sigma^s(\Psi_s), 1) \subset (0,1)$.

PBcomment2

Remark 14. *The assumption* $\mathrm{bi} \leq 3$ *implies the previous one* $\mathrm{bi} \leq 6+4\sqrt{2}$*, which is one reason why we did not try to improve Lemma 10. We do not claim that the assumption* $\mathrm{bi} \leq 3$ *is optimal and it can certainly be improved. Since our data from Table 1 imply that* $\mathrm{bi} \approx 1.786 < 3$*, the assumption of Proposition 13 is satisfied. The same data yield that* $r(\mathrm{bi}) \approx 1.656 > r_{max}(\mathrm{bi}) \approx 1.377$*, so that* $\Psi_s = -\infty$ *and* $\Sigma^s(\Psi)$ *is well defined and increasing on the entire real line* $\mathbb{R}$*. However, as can be seen on Figure 1,* $r(\mathrm{bi})$ *can be smaller than* $r_{max}(\mathrm{bi})$ *for values of* bi *approximately in the interval* $(2,3)$*. The interpretation of* $r(\mathrm{bi})$ *is that the range of values of the screening parameter* Γ *is possibly restricted from* $(0,\Gamma_{max})$ *to* $(0, r(\mathrm{bi})/(\beta\delta))$ *in order to ensure the monotonicity of* $\Sigma^s(\Psi)$ *on the corresponding range of* Ψ*.*

One interest of (52) is to show that the range of admissible values of the potential Ψ *increases up to the entire* $\mathbb{R}$ *as* δ *goes to 0.*

As a matter of fact, the assumption $\mathrm{bi} \leq 3$ *implies that the boundary source nonlinearity in the Poisson-Boltzmann equation* (45) *derives again from a convex energy (cf. Remark 4).*

Proof. From Remark 12 we already know that $\Psi \mapsto \Gamma(\Psi)$ is a decreasing function from $\mathbb{R}$ into its range $(0,\Gamma_{max})$ and thus its inverse $\Psi(\Gamma)$ is well defined from $(0,\Gamma_{max})$ into $\mathbb{R}$. Therefore, replacing Ψ by $\Psi(\Gamma)$ in (44) yields a nonlinear equation in Γ and Σ^s. Since Γ and Σ^s are bounded, while $\Psi(\Gamma)$ and $\ln(\frac{1}{\Sigma^s}-1)$ both vary in the entire real line, equation (44) has always a solution $\Gamma(\Sigma^s)$.

Differentiating (44) with respect to Σ^s yields

$$\left(\frac{d\Psi}{d\Gamma} + \alpha\delta\right)\frac{d\Gamma}{d\Sigma^s} = \frac{\sigma_H \Sigma^s_{max}}{2\mathcal{E}\zeta} + \frac{1}{\Sigma^s(1-\Sigma^s)} > 0. \tag{53}$$

dsSigmader

Therefore, Γ is a monotone decreasing function of Σ^s if and only if $\dfrac{d\Psi}{d\Gamma} + \alpha\delta < 0$. As soon as this monotonicity property is satisfied, there exists a unique solution $\Gamma(\Sigma^s)$ of (44) and the function $\Sigma^s \mapsto \Gamma(\Sigma^s)$ is one-to-one decreasing from $(0,1)$ into $(0,\Gamma_{max})$. Combined with Remark 12 (decreasing character of $\Gamma(\Psi)$) it yields the existence and uniqueness of $\Sigma^s(\Psi)$ which is an increasing function from $\mathbb{R}$ into $(0,1)$.

We study the sign of $\frac{d\Psi}{d\Gamma} + \alpha\delta$. Combining (43) and (49) gives Ψ as a function of Γ

$$\Psi(\Gamma) = -2(\ln\Gamma + \ln(1+\beta\delta\Gamma)) + \alpha\delta\frac{\Gamma}{1+\beta\delta\Gamma} - p(\delta^2 n_H(\Gamma)). \tag{54}$$

PsiGamma

Differentiating (54) with respect to Γ, using the fact that $p'(\xi) > 0$ and the increasing character of $n_H(\Gamma)$ (see Lemma 9) gives

$$\frac{d\Psi}{d\Gamma} + \alpha\delta < -2\frac{1+2\beta\delta\Gamma}{\Gamma(1+\beta\delta\Gamma)} + \frac{\alpha\delta}{(1+\beta\delta\Gamma)^2} + \alpha\delta = \frac{P_3(\beta\delta\Gamma)}{\Gamma(1+\beta\delta\Gamma)^2}.$$

Since $P_3(0) = -2$, $P_3'(0) = 2\mathrm{bi} - 6 \leq 0$ (by assumption) and its leading coefficient is positive, it has one and only one strictly positive root, denoted by $r(\mathrm{bi})$ (which depends only on bi). Thus the quantity $\frac{d\Psi}{d\Gamma} + \alpha\delta$ is negative if $\Gamma < \Gamma_s = r(\mathrm{bi})/(\beta\delta)$. In view of the monotone character of $\Psi(\Gamma)$ (cf. Remark 12), the range $0 \leq \Gamma < \Gamma_s$ is equivalent to the range $\Psi \in (\Psi_s, +\infty)$ with $\Psi_s = \Psi(\Gamma_s)$. Note that, if $\Gamma_{max} < \Gamma_s$, then the condition $\Gamma < \Gamma_s$ is always satisfied and $\Psi_s = -\infty$. Otherwise, a computation, using (54), shows that $\Psi_s = \Psi(\Gamma_s) = 2\ln\delta + C_0$, with the prescribed value of the constant C_0, independent of δ. □

n.smalldelta2

Remark 15. *The regime* $\Psi_s = 2\ln\delta + C_0$ *in Proposition 13 corresponds to* $\Psi_s = \Psi(\Gamma_s)$ *with* $\Gamma_s = r(\mathrm{bi})/(\beta\delta)$*. A simple computation in* (44) *shows that, when* δ *goes to 0,*

$$\Sigma^s(\Psi_s) = C_1\delta^2 + o(\delta^2) \quad \text{with } C_1 = \frac{K^0}{a_H}\exp C_0 + \alpha r(\mathrm{bi})/\beta.$$

sub23

3.2.3 Existence of solutions

The proof of existence of solutions for the MSA model (45) is surprisingly simpler than for the ideal model in Subsection 3.1. The reason is that the non-linearity $n_H(\Psi)$ is now bounded (cf. Lemma 10). Nevertheless, there is still a slight difficulty because, according to Proposition 13, the monotonicity property of the surface density charge Σ^s is valid only for the potential Ψ higher than a threshold value Ψ_s. This requires to define a truncation of $\Sigma^s(\Psi)$ as follows

$$\Sigma^{s,\mathrm{cut}}(z) = \begin{cases} \Sigma^s(z) & \text{for } \Psi_s \le z, \\ \Sigma^s(\Psi_s) & \text{for } z < \Psi_s. \end{cases} \tag{55}$$

Sigcut

We start by studying the corresponding truncated MSA equilibrium problem: find $\Psi_{\mathrm{cut}} \in H^1_{\#}(\Omega_D)$ such that

$$\int_{\Omega_D} \nabla\Psi_{\mathrm{cut}} \cdot \nabla\phi \, dx + \int_{\partial\Omega_D} \tau_B \Sigma^{s,\mathrm{cut}}(\Psi_{\mathrm{cut}})\phi \, ds - \int_{\Omega_D} \tau n_H(\Psi_{\mathrm{cut}})\phi \, dx = 0, \quad \forall \phi \in H^1_{\#}(\Omega_D), \tag{56}$$

VarforiddeltaMSA

where the non-linearities $n_H(\Psi)$ and $\Sigma^s(\Psi)$ are defined by (42), (43) and (44).

istsingleMSA **Proposition 16.** *Assume that* bi ≤ 3. *There exists a unique weak solution* $\Psi_{\mathrm{cut}} \in H^1_{\#}(\Omega_D)$ *of problem (56).*

Proof. First of all, there is no need to assume that the solution belongs to $L^\infty(\Omega_D)$ since the non-linearities $n_H(\Psi)$ and $\Sigma^{s,\mathrm{cut}}(\Psi)$ are bounded. The existence and uniqueness of the solution is classical (see e.g. section 8.2 in [8]) since these non-linearities are monotone, under the assumption bi ≤ 3, according to Lemma 10 and Proposition 13. In particular, as explained in Remark 4, this solution can be obtained by minimizing a strictly convex energy on the space $H^1_{\#}(\Omega_D)$. □

We now construct a subsolution and a supersolution for problem (56).

lem.subsup **Lemma 17.** *Assume that* $\delta < \sqrt{\frac{|\Omega_D|\tau}{|\partial\Omega_D|\tau_B}}$. *Recalling the definition (33) of* U, *define*

$$\underline{\Psi}(x) = \tau_B \left(U(x) - \max_{\overline{\Omega}_D} U \right) + (n_H)^{-1} \left(\frac{|\partial\Omega_D|\tau_B}{|\Omega_D|\tau} \right), \quad x \in \overline{\Omega}_D, \tag{57}$$

subPsiMSA

and, for some $q \in (0,1)$ *such that* $q > \Sigma^s(\Psi_s)$, *define*

$$\overline{\Psi}(x) = \tau_B q \left(U(x) - \min_{\overline{\Omega}_D} U \right) + \max\left\{ (\Sigma^{s,\mathrm{cut}})^{-1}(q), n_H^{-1}(\frac{q|\partial\Omega_D|\tau_B}{|\Omega_D|\tau}) \right\}, \quad x \in \overline{\Omega}_D. \tag{58}$$

superPsiMSA

Then, $\underline{\Psi}$ *is a subsolution and* $\overline{\Psi}$ *is a supersolution for problem (56).*

em.smalldelta **Remark 18.** *The assumption on the smallness of* $\delta = \sqrt{\xi_c}$ *is here to ensure that* $\frac{|\partial\Omega_D|\tau_B}{|\Omega_D|\tau}$ *belongs to the range of* $n_H(\Psi)$ *(cf. Lemma 10). Recall that the limit of* δ *going to zero corresponds to the ideal case (cf. Remark 1). Therefore, it is quite natural to assume such a smallness condition.*

Note that, for q *close to 1,* $q\frac{|\partial\Omega_D|\tau_B}{|\Omega_D|\tau}$ *also belongs to the range of* $n_H(\Psi)$ *and, by virtue of Remark 15, the condition* $q > \Sigma^s(\Psi_s)$ *is always satisfied for small* δ.

Proof. Using definition (33) of U, a direct calculation gives for any $\phi \geq 0,\ \phi \in H^1_{\#}(\Omega_D)$

$$\begin{aligned}&\int_{\Omega_D} \nabla \underline{\Psi} \cdot \nabla \phi \, dx + \int_{\partial\Omega_D} \tau_B \Sigma^{s,\mathrm{cut}}(\underline{\Psi})\phi \, ds - \int_{\Omega_D} \tau n_H(\underline{\Psi})\phi \, dx \\ &= \int_{\partial\Omega_D} \tau_B \big(\Sigma^{s,\mathrm{cut}}(\underline{\Psi}) - 1\big)\phi \, ds + \int_{\Omega_D} \big(\frac{|\partial\Omega_D|}{|\Omega_D|}\tau_B - \tau n_H(\underline{\Psi})\big)\phi \, dx \leq 0, \end{aligned} \tag{59}$$

subcal1MSA

where we used that $\Sigma^{s,\mathrm{cut}} \leq 1$ and the non-positivity of the last integrand follows from the bound

$$\underline{\Psi}(x) \leq (n_H)^{-1}\left(\frac{|\partial\Omega_D|\tau_B}{|\Omega_D|\tau}\right)$$

and the decreasing character of $\Psi \mapsto n_H(\Psi)$. Hence the function $\underline{\Psi}$ is a subsolution for problem (56).

Arguing as in (37), the monotonicity of Σ^s and n_H yields for any $\phi \geq 0,\ \phi \in H^1_{\#}(\Omega_D)$

$$\begin{aligned}&\int_{\Omega_D} \nabla \overline{\Psi} \cdot \nabla \phi \, dx + \int_{\partial\Omega_D} \tau_B \Sigma^{s,\mathrm{cut}}(\overline{\Psi})\phi \, ds - \int_{\Omega_D} \tau n_H(\overline{\Psi})\phi \, dx \\ &= \int_{\partial\Omega_D} \tau_B \big(\Sigma^{s,\mathrm{cut}}(\overline{\Psi}) - q\big)\phi \, ds + \int_{\Omega_D} \big(\frac{|\partial\Omega_D|}{|\Omega_D|}\tau_B q - \tau n_H(\overline{\Psi})\big)\phi \, dx \geq 0. \end{aligned} \tag{60}$$

superX2

Indeed, since $\overline{\Psi}(x) \geq (\Sigma^{s,\mathrm{cut}})^{-1}(q)$, by monotonicity of $\Sigma^{s,\mathrm{cut}}$ we obtain

$$\Sigma^{s,\mathrm{cut}}(\overline{\Psi}) \geq \Sigma^{s,\mathrm{cut}}\left((\Sigma^{s,\mathrm{cut}})^{-1}(q)\right) \geq q,$$

and, since $\overline{\Psi}(x) \geq n_H^{-1}(\frac{q|\partial\Omega_D|\tau_B}{|\Omega_D|\tau})$ in $\overline{\Omega}_D$, by monotonicity of $n_H(\Psi)$ we deduce

$$\frac{|\partial\Omega_D|}{|\Omega_D|}\tau_B q - \tau n_H(\overline{\Psi}) \geq \frac{|\partial\Omega_D|}{|\Omega_D|}\tau_B q - \tau n_H(n_H^{-1}(\frac{q|\partial\Omega_D|\tau_B}{|\Omega_D|\tau})) = 0.$$

It yields that $\overline{\Psi}$ is a supersolution for problem (56). □

We are now in a position to study the variational formulation of the original MSA problem (15): find $\Psi \in H^1_{\#}(\Omega_D)$ such that

$$\int_{\Omega_D} \nabla\Psi \cdot \nabla\phi \, dx + \int_{\partial\Omega_D} \tau_B \Sigma^s(\Psi)\phi \, ds - \int_{\Omega_D} \tau n_H(\Psi)\phi \, dx = 0, \quad \forall \phi \in H^1_{\#}(\Omega_D), \tag{61}$$

VarforiddeltaMSA2

TrueexistMSA **Theorem 19.** *For sufficiently small $\delta > 0$, the weak solution Ψ_{cut} of (56) is also the unique solution $\Psi = \Psi_{\mathrm{cut}}$ of (61) in $H^1_{\#}(\Omega_D)$, satisfying the same bounds $\underline{\Psi} \leq \Psi \leq \overline{\Psi}$.*

Proof. A solution for the truncated problem (56) would also solve (61) if $\Psi_s \leq \min_x \underline{\Psi}$ because, in such a case, the truncation is inoperative. Using definition (52) of Ψ_s, the later holds true if

$$\frac{2}{z_H}\ln\delta + C_0 \leq \tau_B(\min_{\overline{\Omega}_D} U - \max_{\overline{\Omega}_D} U) + (n_H)^{-1}\big(\frac{|\partial\Omega_D|\tau_B}{|\Omega_D|\tau}\big),$$

which is certainly true for sufficiently small δ (this condition can be made more explicit). □

4 Mathematical analysis with several ions

s.2ions

This section investigates the existence of solutions for the nonlinear boundary value problem (26) in the case of several ions. As in the case of a single ion, we start by studying the ideal case which has a nicer monotone structure. Afterwards, we consider the MSA case which is somehow simpler because the non-linearities are bounded. Nevertheless, we loose uniqueness of the solutions since the MSA model lacks monotonicity.

4.1 Ideal model with several ions

ss.2ideal

As in Subsection 2.3 we consider a solution of N different ions in water, labelled by an index $i \in \{1, ..., N\}$, with valence z_i, constant activity a_i and concentration n_i. We restrict ourselves to the ideal case, meaning that the ion activity coefficients are $\gamma_i = 1$. We perform an adimensionalization, similar to that of Subsection 3.1,

$$n_i^{id}(x) = a_H \tilde{n}_i^{id}(\tilde{x}), \quad a_i = a_H \tilde{a}_i, \quad \Psi(x) = \zeta \tilde{\Psi}(\tilde{x}) \quad \text{and} \quad \Sigma_{id}^s(x) = \Sigma_{max}^s \tilde{\Sigma}_{id}^s(\tilde{x}), \tag{62}$$

multi.adim

where a_H is a characteristic value of the activity of H^+. After dropping tildes, we introduce

$$N^{id}(\Psi) = \sum_{i=1}^{N} z_i n_i(\Psi) \quad \text{with } n_i(\Psi) = a_i e^{-z_i \Psi}.$$

The surface charge Σ_{id}^s is still defined by (28) and, in particular, $\Psi \mapsto \Sigma_{id}^s(\Psi)$ is monotone increasing from $\mathbb{R}$ into $(0, 1)$, according to Lemma 3. The system (26) becomes in the adimensional ideal case

$$\begin{cases} -\Delta\Psi = \tau \displaystyle\sum_{i=1}^{N} z_i n_i(\Psi) & \text{in} \quad \Omega_D, \\ \nabla\Psi \cdot \nu = -\tau_B \Sigma_{id}^s(\Psi) & \text{on} \quad \partial\Omega_D, \\ x \mapsto \Psi(x) & \text{is } (0,1)^d\text{-periodic}, \end{cases} \tag{63}$$

Eqmultia

where τ and τ_B are defined by (27). The existence and uniqueness of a solution to (63) is quite similar to the case of a single ion in Subsection 3.1. The variational formulation of problem (63) is: find $\Psi \in H^1_{\#}(\Omega_D) \cap L^\infty(\Omega_D)$, such that

$$\int_{\Omega_D} \nabla\Psi \cdot \nabla\phi \, dx + \int_{\partial\Omega_D} \tau_B \Sigma_{id}^s(\Psi)\phi \, ds - \int_{\Omega_D} \tau N^{id}(\Psi)\phi \, dx = 0, \quad \forall \phi \in H^1_{\#}(\Omega_D). \tag{64}$$

Varforidmulti

Note that the solution is required to be bounded so that the nonlinear term involving $N^{id}(\Psi)$ is integrable.

lem.decr

Lemma 20. *The function $N^{id}(\Psi)$ is monotone decreasing on $\mathbb{R}$.*

Remark 21. *According to Remark 2, there is at least one $z_i > 0$, so the range of $N^{id}(\Psi)$ contains $\mathbb{R}^+$. In most practical cases, as we assumed, the solution contains both anions and cations, that is positive and negative values of the valences z_i, and thus the range of $N^{id}(\Psi)$ is $\mathbb{R}$. However, if all valences were positive, then the range of $N^{id}(\Psi)$ would be just $\mathbb{R}^+$.*

Proof. A simple computation shows that

$$(N^{id})'(\Psi) = \sum_{i=1}^{N} -z_i^2 a_i e^{-z_i \Psi} < 0.$$

Similarly, a primitive of $-N^{id}(\Psi)$ is

$$\sum_{i=1}^{N} a_i e^{-z_i \Psi},$$

which is a convex function of Ψ. □

By virtue of Lemma 20, Remark 4 still applies, meaning that (64) is the Euler-Lagrange equation for the minimization of a convex energy.

multiexist **Theorem 22.** *There exists a unique solution $\Psi \in H^1_{\#}(\Omega_D) \cap L^\infty(\Omega_D)$ of problem (64).*

The proof of Theorem 22 requires to first introduce a cut-off function for N^{id}. For $M > 0$ define

$$N^{id}_M(z) = \begin{cases} N^{id}(z) & \text{for } -M \le z \le M, \\ N^{id}_M(-M) & \text{for } z < -M, \\ N^{id}_M(M) & \text{for } M < z. \end{cases} \tag{65}$$ nhcutoffidmulti

The truncated version of (64) reads: find $\Psi_M \in H^1_{\#}(\Omega_D)$ such that

$$\int_{\Omega_D} \nabla \Psi_M \cdot \nabla \phi \, dx + \int_{\partial \Omega_D} \tau_B \Sigma^s_{id}(\Psi_M) \phi \, ds - \int_{\Omega_D} \tau N^{id}_M(\Psi_M) \phi \, dx = 0, \quad \forall \phi \in H^1_{\#}(\Omega_D). \tag{66}$$ Varforiddeltamulti

First, we construct a subsolution and a supersolution for problem (66). Recall that $U(x)$ is the solution of the auxiliary Neumann problem (33).

lem.subsup2 **Lemma 23.** *Define, for $x \in \overline{\Omega}_D$,*

$$\underline{\Psi}(x) = \tau_B \left((U(x) - \max_{\overline{\Omega}_D} U \right) + (N^{id})^{-1} \left(\frac{|\partial \Omega_D| \tau_B}{|\Omega_D| \tau} \right), \tag{67}$$ subPsimulti

and

$$\overline{\Psi}(x) = \frac{\tau_B}{2} \left(U(x) - \min_{\overline{\Omega}_D} U \right) + \max \left((\Sigma^s_{id})^{-1}(\frac{1}{2}), (N^{id})^{-1}(\frac{|\partial \Omega_D| \tau_B}{2|\Omega_D| \tau}) \right). \tag{68}$$ superPsimulti

Assume

$$M > (N^{id})^{-1}(\frac{|\partial \Omega_D| \tau_B}{2|\Omega_D| \tau}). \tag{69}$$ sizeM

Then, $\underline{\Psi}$ is a subsolution and $\overline{\Psi}$ is a supersolution for problem (66).

Proof. The calculation is analogous to (36): for any $\phi \ge 0$, $\phi \in H^1_{\#}(\Omega_D)$

$$\begin{aligned} &\int_{\Omega_D} \nabla \underline{\Psi} \cdot \nabla \phi \, dx - \tau \int_{\Omega_D} N^{id}_M(\underline{\Psi}) \phi \, dx + \tau_B \int_{\partial \Omega_D} \Sigma^s_{id}(\underline{\Psi}) \phi \, ds = \\ &\tau_B \int_{\partial \Omega_D} \big(\Sigma^s_{id}(\underline{\Psi}) - 1 \big) \phi \, ds + \int_{\Omega_D} \big(\frac{|\partial \Omega_D| \tau_B}{|\Omega_D|} - \tau N^{id}_M(\underline{\Psi}) \big) \phi \, dx \le 0, \end{aligned} \tag{70}$$ subcal1multi

because, since N^{id}_M is decreasing and $M \ge (N^{id})^{-1}(\frac{|\partial \Omega_D| \tau_B}{|\Omega_D| \tau})$,

$$N^{id}_M(\underline{\Psi}) \ge N^{id}_M(\max_{x \in \Omega_D} \underline{\Psi}) = N^{id}_M((N^{id})^{-1}(\frac{|\partial \Omega_D| \tau_B}{|\Omega_D| \tau})) = N^{id}((N^{id})^{-1}(\frac{|\partial \Omega_D| \tau_B}{|\Omega_D| \tau})) = \frac{|\partial \Omega_D| \tau_B}{|\Omega_D| \tau}.$$

We conclude that $\underline{\Psi}$ is a subsolution for problem (66).

Again we use definition of U and the strict monotonicity of Σ^s_{id} and it is enough to go through the calculation at the last line of (37). It yields, for any $\phi \geq 0,\ \phi \in H^1_{\#}(\Omega_D)$

$$\int_{\Omega_D} \nabla\overline{\Psi}\cdot\nabla\phi\ dx - \int_{\Omega_D} \tau N^{id}_M(\overline{\Psi})\phi\ dx + \int_{\partial\Omega_D} \tau_B \Sigma^s_{id}(\overline{\Psi})\phi\ ds = \tag{71}$$

$$\int_{\partial\Omega_D} \big(\Sigma^s_{id}(\overline{\Psi}) - \frac{1}{2}\big)\phi\ ds + \int_{\Omega_D} \big(\frac{|\partial\Omega_D|}{2|\Omega_D|}\tau_B - \tau N^{id}_M(\overline{\Psi})\big)\phi\ dx \geq 0, \tag{72}$$

superXmulti

because, for the first term in the right hand side of (72), $\overline{\Psi}(x) \geq (\Sigma^s_{id})^{-1}(\frac{1}{2})$ and Σ^s_{id} is increasing, while for the second term, $\overline{\Psi}(x) \geq (N^{id})^{-1}(\frac{|\partial\Omega_D|\tau_B}{2|\Omega_D|\tau})$ and $N^{id}_M(\Psi)$ is decreasing so that

$$\tau N^{id}_M(\overline{\Psi}) \leq \tau N^{id}_M((N^{id})^{-1}(\frac{|\partial\Omega_D|\tau_B}{2|\Omega_D|\tau})) = \tau N^{id}((N^{id})^{-1}(\frac{|\partial\Omega_D|\tau_B}{2|\Omega_D|\tau})) = \frac{|\partial\Omega_D|}{2|\Omega_D|}\tau_B.$$

Hence $\overline{\Psi}$ is a supersolution for problem (66). □

Having found a subsolution and a supersolution, and since N^{id}_M and Σ^s_{id} are bounded and monotone, the existence and uniqueness of a solution $\Psi_M \in H^1_{\#}(\Omega_D)\cap L^\infty(\Omega_D)$ of (66) is classical, as already explained for Proposition 8.

Proof of Theorem 22. Since the solution Ψ_M of (66) satisfies

$$\underline{\Psi} \leq \Psi_M \leq \overline{\Psi},$$

choosing M large enough implies that $N^{id}_M(\Psi_M) = N^{id}(\Psi_M)$ and, as a consequence, $\Psi = \Psi_M$ is a solution for problem (64). By the strict monotonicity of the nonlinearities N^{id} and Σ^s_{id}, the solution is unique. Therefore, problem (64) has a unique solution in $H^1_{\#}(\Omega_D)\cap L^\infty(\Omega_D)$, □

4.2 MSA equilibrium solution in the multiple ion case

sub33

We first perform an adimensionalization of the equations of Subsection 2.3, mixing arguments from Subsections 3.2.1 and 4.1. Without entering too much into details, we introduce the adimensional unknowns (62), as well as the characteristic values (38), (39) and (40). Defining a non-linear function N for the electrical charge density

$$N(\Psi) = \sum_{i=1}^{N} z_i n_i(\Psi),$$

it yields the following system

$$\begin{cases} -\Delta\Psi = \tau N(\Psi) & \text{in} \quad \Omega_D, \\ \nabla\Psi\cdot\nu = -\tau_B\Sigma^s(\Psi) & \text{on} \quad \partial\Omega_D, \\ x \mapsto \Psi(x) & \text{is } (0,1)^d\text{-periodic}, \end{cases} \tag{73}$$

Eqmultimsa

where τ and τ_B are defined by (27), the surface charge, $0 \leq \Sigma^s(\Psi) \leq 1$ is defined by the adimensionalized version of (14), i.e.,

$$\Psi = \frac{\sigma_H\Sigma^s_{max}}{2\mathcal{E}\zeta}\Sigma^s - \alpha\delta\Gamma - \ln(\frac{1}{\Sigma^s} - 1) - \ln\frac{K^0}{a_H}, \tag{74}$$

Sigmadim

while the ion density is given by the adimensionalized version of (25), together with (21) and (23), i.e.,

$$n_i(\Psi) = a_i e^{-z_i\Psi} e^{\frac{\alpha\delta\Gamma z_i^2}{1+\beta\delta\Gamma}} e^{-p\left(\delta^2 N_0(\Psi)\right)} \quad \text{with} \quad N_0(\Psi) = \sum_{j=1}^{N} n_j(\Psi). \tag{75}$$

ni.msa

Recall that α and β are defined in (40) and that $\delta = \sqrt{\xi_c}$ is a small parameter. It remains to define the MSA screening parameter Γ. To simplify the analysis, we make the assumption that all ions have the same diameter, namely $\sigma_i = \sigma_H$ for any i. Such an hypothesis was already made in [2] for a seemingly different reason (proving the well-posedness of the linearization of (73)) and thus is both not unusual and fundamentally important. Since the diameters of all ions are assumed to be equal, $\sigma_i = \sigma_H$ for any i, equation (22) defining the MSA screening parameter has a unique positive root, given by

$$\Gamma = \frac{2\sqrt{N_2(\Psi)}}{1+\sqrt{1+4\beta\delta\sqrt{N_2(\Psi)}}} \quad \text{with} \quad N_2(\Psi) = \sum_{i=1}^{N} z_i^2 n_i(\Psi) \tag{76}$$

rootGamma2

Eventually, the MSA model is the combination of system (73) with the algebraic equations (74), (75) and (76). We first prove that these nonlinear algebraic equations have a solution, namely that, for a given value $\Psi \in \mathbb{R}$, they allow us to compute the ion densities $n_i(\Psi)$ and the surface charge $\Sigma^s(\Psi)$.

lem.N0 **Lemma 24.** *The algebraic equations* (75) *and* (76) *define functions* $\Psi \mapsto n_i(\Psi)$*, for* $1 \le i \le N$*. Furthermore, the function* $N_0(\Psi)$*, defined in* (75)*, takes values in* $(0, \delta^{-2})$*.*

rem.N0 **Remark 25.** *Lemma 24 does not say anything about uniqueness of the solution to the nonlinear algebraic equations* (75) *and* (76)*. Its proof explains which solution is chosen.*

Proof. Summing (75) over i leads to

$$N_0(\Psi) = e^{-p\left(\delta^2 N_0(\Psi)\right)} \sum_{i=1}^{N} a_i e^{-z_i\Psi} e^{\frac{\alpha\delta\Gamma z_i^2}{1+\beta\delta\Gamma}}. \tag{77}$$

N0

Multiplying (75) by z_i^2 and summing over i leads to

$$N_2(\Psi) = e^{-p\left(\delta^2 N_0(\Psi)\right)} \sum_{i=1}^{N} z_i^2 a_i e^{-z_i\Psi} e^{\frac{\alpha\delta\Gamma z_i^2}{1+\beta\delta\Gamma}}$$

which can be rewritten as

$$N_2(\Psi) = N_0(\Psi) \frac{\displaystyle\sum_{i=1}^{N} z_i^2 a_i e^{-z_i\Psi} e^{\frac{\alpha\delta\Gamma z_i^2}{1+\beta\delta\Gamma}}}{\displaystyle\sum_{i=1}^{N} a_i e^{-z_i\Psi} e^{\frac{\alpha\delta\Gamma z_i^2}{1+\beta\delta\Gamma}}}. \tag{78}$$

N2

Equations (77) and (78) form a system of two equations for the two unknowns $N_0(\Psi)$ and $N_2(\Psi)$, depending on the parameter Ψ. From (76) Γ is clearly a function of $N_2(\Psi)$ only, namely $\Gamma = \Gamma(N_2(\Psi))$ in (77) and (78). Fix any values of $\Psi \in \mathbb{R}$ and $N_2(\Psi) \in \mathbb{R}$ and consider (77) as a nonlinear fixed point equation for the unknown $N_0(\Psi)$. Since, in view of the definition (23) of $p(\xi)$ for $\xi \in (0,1)$, $p'(\xi) = \frac{8-2\xi}{(1-\xi)^4} > 0$, the map $\zeta \mapsto e^{-p\left(\delta^2\zeta\right)}$ is strictly decreasing from $(0, \delta^{-2})$ into its

range, we deduce the uniqueness of a solution $N_0(\Psi)$, as well as the bound $0 \leq N_0(\Psi) \leq \delta^{-2}$. Plug this value of $N_0(\Psi)$ (which depends on Ψ and $N_2(\Psi)$) in (78) which is now a nonlinear equation for $N_2(\Psi)$ in terms of Ψ. The right hand side of (78) is a very complicated continuous function of Ψ and $N_2(\Psi)$, but it is bounded by $\delta^{-2} \max_i z_i^2$. On the contrary, the left hand side of (78) is linear increasing in $N_2(\Psi)$. Therefore, starting from 0, if the value of $N_2(\Psi)$ is increased, there is always a first root of (78). We choose this solution (there may be other ones larger but still less than $\delta^{-2} \max_i z_i^2$). Having determined $N_0(\Psi)$ and $N_2(\Psi)$ as functions of Ψ, (75) defines $n_i(\Psi)$ as a function solely of Ψ. □

rem.Sima **Remark 26.** *In the special case of $N = 2$ ions with opposite valences $z_1 = -z_2$, Lemma 24 can be slightly improve. Indeed, in such a case, $N_2(\Psi) = z_1^2 N_0(\Psi)$ and rewriting* (77) *as*

$$N_0(\Psi) e^{p\left(\delta^2 N_0(\Psi)\right)} e^{-\frac{\alpha \delta \Gamma z_1^2}{1+\beta\delta\Gamma}} = \sum_{i=1}^{2} a_i e^{-z_i \Psi},$$

one can prove that the left hand side is a monotone increasing function of $N_0(\Psi)$, at least if the Bjerrum parameter satisfies $\mathrm{bi} \leq 4(1+\sqrt{2})^2/z_1^2$ *(the proof involves similar arguments as in Proposition 29 below). Therefore, the nonlinear algebraic equations* (75) *and* (76) *have a unique solution.*

lem.Sigma **Lemma 27.** *The algebraic equation* (74) *uniquely defines a function $\Psi \mapsto \Sigma^s(\Psi)$, from $\mathbb{R}$ into $(0,1)$.*

Proof. Rewrite (74) as

$$\frac{\sigma_H \Sigma^s_{max}}{2\mathcal{E}\zeta} \Sigma^s - \ln(\frac{1}{\Sigma^s} - 1) = \Psi + \alpha\delta\Gamma + \ln \frac{K^0}{a_H}$$

where the right hand side is a function of Ψ, as a consequence of Lemma 24. It is easily seen that the left hand side is a strictly increasing function of Σ^s from $(0,1)$ into $\mathbb{R}$. Therefore, it admits a unique solution $\Sigma^s(\Psi)$. □

thm.Sigma **Theorem 28.** *The MSA model* (73)*, with the algebraic equations* (74)*,* (75) *and* (76)*, admits a solution $\Psi \in H^1_{\#}(\Omega_D)$.*

Proof. As a consequence of Lemma 24 the non-linearity in the right hand side of (73) is uniformly bounded for any $\Psi \in H^1_{\#}(\Omega_D)$ since

$$|N(\Psi)| \leq \max_{1\leq i\leq N} |z_i| N_0(\Psi) \leq \delta^{-2} \max_{1\leq i\leq N} |z_i|.$$

Similarly the non-linear boundary condition $\Sigma^s(\Psi)$ is bounded between 0 and 1, by definition. Then, under these conditions the existence of at least one solution is classical by using a fixed point argument (see e.g. chapter 9 in [8]). □

Theorem 28 does not say anything on the uniqueness of solutions of the MSA model (73). Contrary, to the ideal case of Subsection 4.1 we are unable to prove uniqueness of the solution, even under additional assumptions on the physical parameters. Actually, we can only prove the monotonicity of the charge density $N(\Psi)$ but not of the surface charge $\Sigma^s(\Psi)$ (Lemma 27 does not say anything about its monotonicity).

monotoneN **Proposition 29.** *Assume the Bjerrum parameter* $\mathrm{bi} = L_B/\sigma_H$ *satisfies the upper bound*

$$\mathrm{bi} \max_{1\le i\le N} z_i^2 \le 4(1+\sqrt{2})^2.$$

Then, $\Psi \mapsto N(\Psi)$ *is a strictly monotone decreasing function on* $\mathbb{R}$.

rem.monotoneN **Remark 30.** *For a solution of* $Ca(OH)_2$*, as studied in the numerical section, since* $\max_{1\le i\le N} z_i^2 = 4$ *and* $\mathrm{bi} \approx 1.786$*, according to the data of Table 1, the assumption of Proposition 29 is satisfied.*

Proof. Taking the logarithm of the definition (75) of n_i yields

$$\ln n_i = -z_i\Psi + \ln a_i + \frac{\alpha\delta\Gamma z_i^2}{1+\beta\delta\Gamma} - p\left(\delta^2 N_0(\Psi)\right). \tag{79}$$ logequilsansdmult

Differentiating (79) with respect to Ψ yields

$$\frac{1}{n_i}\frac{dn_i}{d\Psi} = -z_i + \frac{\alpha\delta z_i^2}{(1+\beta\delta\Gamma)^2}\frac{d\Gamma}{d\Psi} - \delta^2 p'\left(\delta^2 N_0(\Psi)\right)\sum_{j=1}^N \frac{dn_j}{d\Psi} =$$

$$-z_i + \sum_{j=1}^N \frac{dn_j}{d\Psi}\left(-\delta^2 p'\left(\delta^2 N_0(\Psi)\right) + \frac{\alpha\delta z_i^2 z_j^2}{2(1+\beta\delta\Gamma)^2(1+2\beta\delta\Gamma)\sqrt{N_2(\Psi)}}\right), \tag{80}$$ Dervni

since differentiating (76) (and using the proof of Lemma 9) leads to

$$\frac{d\Gamma}{d\Psi} = \frac{d\Gamma}{d\sqrt{N_2}}\frac{d\sqrt{N_2}}{dN_2}\frac{dN_2}{d\Psi} = \frac{1}{1+2\beta\delta\Gamma}\frac{1}{2\sqrt{N_2}}\sum_{i=1}^N z_i^2\frac{dn_i}{d\Psi}.$$

Therefore, (80) is equivalent to the linear system

$$\mathcal{A}\left(\frac{dn_i}{d\Psi}\right)_{i=1,\dots,N} = (-z_i)_{i=1,\dots,N}, \tag{81}$$ linsyst

where $\mathcal{A}$ is a $N\times N$ symmetric matrix defined by its entries

$$\mathcal{A}_{ij} = \frac{\delta_{ij}}{n_i} + \delta^2 p'\left(\delta^2 N_0(\Psi)\right) - \frac{\alpha\delta z_i^2 z_j^2}{2(1+\beta\delta\Gamma)^2(1+2\beta\delta\Gamma)\sqrt{N_2(\Psi)}}, \tag{82}$$ linsyst2

where δ_{ij} is the Kronecker symbol. If $\mathcal{A}$ is invertible, then

$$\frac{dN}{d\Psi} = -\mathcal{A}^{-1}(z_i)_{i=1,\dots,N}\cdot(z_i)_{i=1,\dots,N}$$

and the decreasing character of $N(\Psi)$ is proved if $\mathcal{A}^{-1}$ is positive. This is equivalent to prove that $\mathcal{A}$ is positive definite. For any vector $y = (y_i)_{i=1,\dots,N}$, compute

$$\mathcal{A}y\cdot y = \sum_{i=1}^N \frac{y_i^2}{n_i} + \delta^2 p'\left(\delta^2 N_0(\Psi)\right)\left(\sum_{i=1}^N y_i\right)^2 - \frac{\alpha\delta\left(\sum_{i=1}^N z_i^2 y_i\right)^2}{2(1+\beta\delta\Gamma)^2(1+2\beta\delta\Gamma)\sqrt{N_2(\Psi)}}$$

$$\ge \|\tilde{y}\|^2\left(1 - \frac{\alpha\delta\left(\sum_{i=1}^N z_i^4 n_i\right)}{2(1+\beta\delta\Gamma)^2(1+2\beta\delta\Gamma)\sqrt{N_2(\Psi)}}\right) \ge \|\tilde{y}\|^2\left(1 - \frac{\alpha\delta\sqrt{N_2(\Psi)}\max_{1\le i\le N} z_i^2}{2(1+\beta\delta\Gamma)^2(1+2\beta\delta\Gamma)}\right),$$

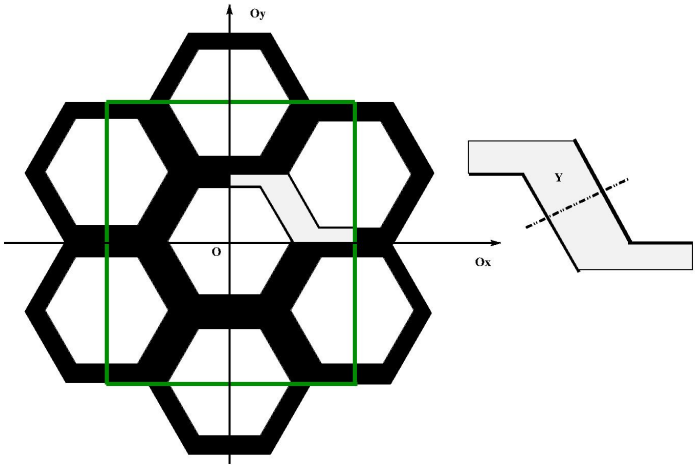

Figure 2: The periodic domain Q in green with its solid part (in white) and its pore volume Ω_D (in black). By symmetry all calculations are performed in the smaller set Y (right). fig.pore

because $p'(\xi) \geq 0$ and using the change of variables $\tilde{y}_i = y_i/\sqrt{n_i}$ with Cauchy-Schwarz inequality. Recalling definition (76) of Γ and introducing a new variable $t = \sqrt{1 + 4\beta\delta\sqrt{N_2(\Psi)}}$ leads to

$$\mathcal{A}y \cdot y \geq \|\tilde{y}\|^2 \, (1 - f(t)) \qquad \text{with} \qquad f(t) = \frac{(t-1)\alpha \max_{1 \leq i \leq N} z_i^2}{4\beta t(1+t)}.$$

Some simple optimization with respect to $t \in (1; +\infty)$ yields the desired result because $\mathrm{bi} = \alpha/\beta$. □

5 Numerical results

s.num

5.1 Geometrical setting

We consider a periodic domain in the plane ($d = 2$) for which the pore or fluid part Ω_D is a honeycomb. Because of this special structure, the periodic domain is not a square but a rectangle $Q = (0, L_x) \times (0, L_y)$ with dimensions $L_x = 652\ nm$ and $L_y = 723\ nm$ (see the green rectangle in Figure 2). In the middle of the cell, the solid part (in white) is a hexagon of width 200 nm, while the fluid channels (in black) have a cross-section of width 30 nm. Because of mirror symmetries with respect to the vertical and horizontal axes, the fluid domain Ω_D can be restricted to the subset denoted by Y on Figure 2. The boundary ∂Y is composed of the solid/pore interface $\partial\Omega_D$, where the non-linear boundary condition takes place, and its complement ∂Y_0, where homogeneous Neumann boundary condition are imposed for symmetry reasons. Because of these symmetries, no periodic boundary conditions have to be enforced. This subset Y is the computational domain, meshed by $61,334$ triangles with a mesh refinement near the solid/pore interface. The number of degree of freedom is $136,987$. All our numerical results are obtained with the `FreeFem++` package [11], using Lagrange $\mathbb{P}_2$ finite elements. The dashed axis shown on the right of Figure 2 is placed right in the middle of the channel and it is where the cross-sections of the potential are plotted (see below).

5.2 Newton algorithm

To solve the non-linear partial differential equation (73) we use a Newton algorithm which is briefly recalled. Because of the geometric setting, (73) boils down to

$$\left\{\begin{array}{lcll} -\Delta\Psi & = & \tau\, N(\Psi) & \text{in} \quad Y, \\ \nabla\Psi\cdot\nu & = & -\tau_B\,\Sigma^s(\Psi) & \text{on } \partial\Omega_D, \\ \nabla\Psi\cdot\nu & = & 0 & \text{on } \partial Y\setminus\partial\Omega_D. \end{array}\right.$$

Define its variational form

$$R(\Psi,v)=\int_Y \nabla\Psi\cdot\nabla v\,dx+\tau_B\int_{\partial\Omega_D}\Sigma^s(\Psi)\,v\,ds-\tau\int_Y N(\Psi)\,v\,dx$$

and its differential

$$D_\Psi R(\Psi,v)[\delta\Psi]=\int_Y \nabla\delta\Psi\cdot\nabla v\,dx+\tau_B\int_{\partial\Omega_D}\frac{d\Sigma^s}{d\Psi}(\Psi)\,v\,ds-\tau\int_Y\frac{dN}{d\Psi}(\Psi)\,v\,dx\,.$$

The formulas for the derivatives are implicitly given in the theoretical analysis of the previous sections. If $\Psi^{(0)}$ is some initialization for the potential Ψ, a sequence of approximate solutions is defined by

$$\Psi^{(n)} \;=\; \Psi^{(n-1)} \;+\; \delta\Psi$$

where $\delta\Psi$ is the solution of the linear equation

$$D_\Psi R(\Psi^{(n-1)},v)[\delta\Psi] \;=\; -R(\Psi^{(n-1)},v) \qquad \forall\; v\in H^1\,(Y)\,.$$

Convergence is detected when the relative residual $\|\delta\Psi\|/\|\Psi^{(n-1)}\|$, computed in the $H^1(Y)$-norm, is smaller than 10^{-7}. Furthermore, the electroneutrality between the bulk and surface charges is checked.

5.3 Numerical results for the single ion case

ss.singnum

We first perform a numerical computation for system (45) for the single H^+ ion in the MSA case. We choose $pH=7$ meaning that the activity is $a_H=1.e-7$ mole/liter (see Table 1). Figure 3 shows the isovalues of the potential Ψ, the maxima of which are located at the pore junctions. It is interesting to see if there is a noticeable difference with the same computation performed with a constant surface charge density Σ^{av}, defined by

$$\Sigma^{av}=\frac{1}{|\partial\Omega_D|}\int_{\partial\Omega_D}\Sigma^s(\Psi)ds. \tag{83}$$

eq.average

Figure 4 shows the difference between the surface charge density Σ^s obtained with the nonlinear boundary condition for a $pH=7$ and its average Σ^{av} on the boundary. The variation of Σ^s around its average Σ^{av} is of the order of one percent. The plot on Figure 4 is along the lower left solid boundary of Y, which exhibits two corners where the surface charge density has clearly a peak.

For the sake of comparison, we thus perform the same computation as for Figure 3, except that the non-linear boundary condition $\Sigma^s(\Psi)$ is replaced by the constant Neumann boundary condition Σ^{av}. The difference between the potential Ψ in these two cases is plotted on Figure 5 where it can be checked that the relative difference is very small, less than $5.e^{-5}$. This is confirmed by the

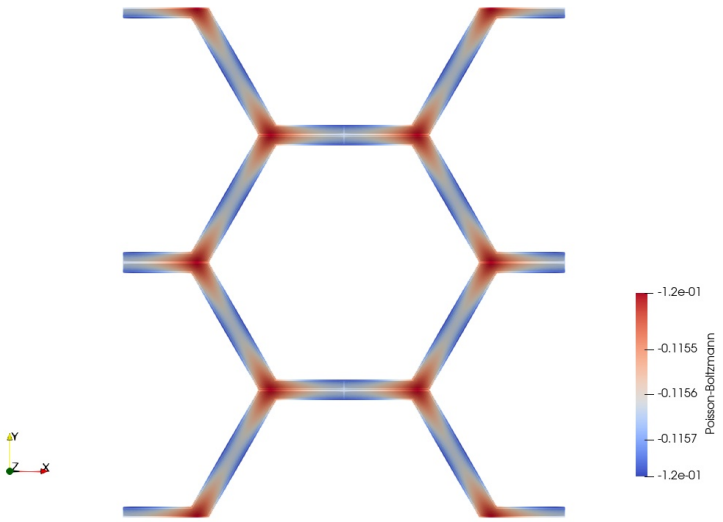

Figure 3: Isovalues of Ψ (Volts) for a single ion with $pH = 7$ in the MSA case. `fig.isoH+`

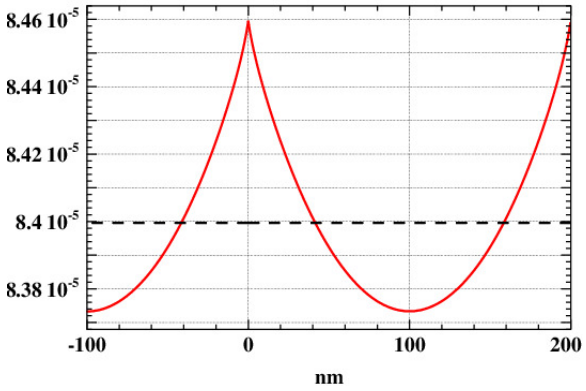

Figure 4: Surface charge density Σ^s (eC/nm^2) on the lower left part of the boundary of Y for $pH = 7$ in MSA case. The dotted line shows its mean value Σ^{av}. `fig.SigmaMSAetCst`

comparison on Figure 6 of the two profiles of the potential Ψ along a cross-section of a channel (cf. the dashed line on the right of Figure 2), which are very close. For completeness, we plot on Figure 7 the profile of Ψ for the MSA model on two cross-sections: one in the middle of the channel (as in Figure 6) and the other at the extremity of the channel. The higher value of Ψ at the end rather than at the middle of the channel is consistent with the peak of $\Sigma^s(\Psi)$ at the corners or end points of the fluid channels.

We now perform some comparisons between the ideal and MSA models as a function of pH varying from 1 to 14. Note that the single ion model was established for $pH = 7$ but it makes sense, at least from a numerical point of view, to test its numerical output when the pH varies. The activity a_H of the H^+ ion is equal to 10^{-pH} (mole/liter). The coefficient $\tau = (L/\lambda_D)^2$ takes into account the

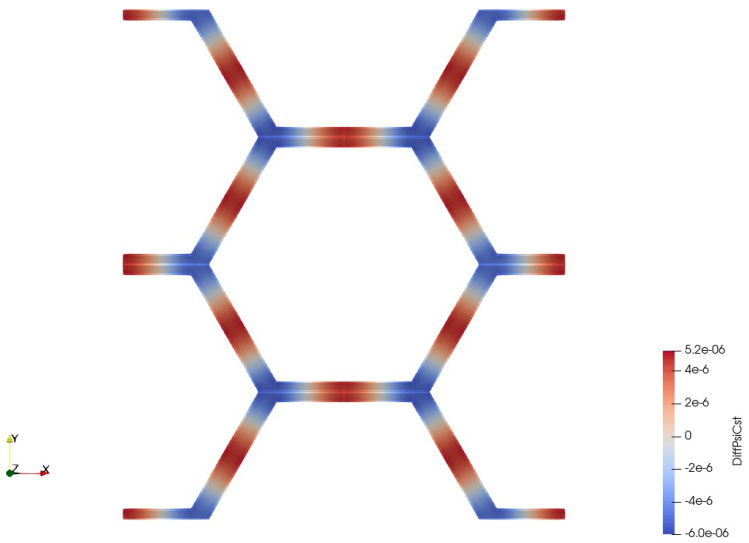

Figure 5: Isovalues of the differences in Ψ (Volts), computed with the non-linear boundary condition $\Sigma^s(\Psi)$ and its constant average Σ^{av}, for a single ion with $pH = 7$ in the MSA case.

`fig.isodiffH+`

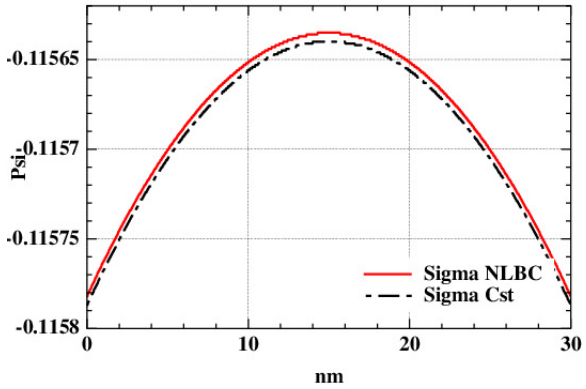

Figure 6: Cross-sections of the Potentials Ψ ($Volts$) for the non-linear boundary condition (**NLBC**) $\Sigma^s(\Psi)$ and for its constant average (**Cst**) Σ^{av} with $pH = 7$ in the MSA case.

`fig.PBSigmaMSAetCst-`

different values of the pH via the Debye's length λ_D which depends on a_H (see Table 1). It turns out that there is almost no differences between the calculations of the two models, ideal and MSA, whatever the value of pH. The reason is the very low salt concentration. Actually here the bulk salt concentration is nill. Nevertheless, we can observe on Figure 8 the linear variation of the maximums of Ψ as a function of the pH. There is a change of sign of the potential maximum between the values 5.041 and 5.042 of the pH for the Ideal and MSA cases, see Figure 9. All cross-sections of potentials obtained for other values of pH have roughly the same profile as those shown in Figure 9.

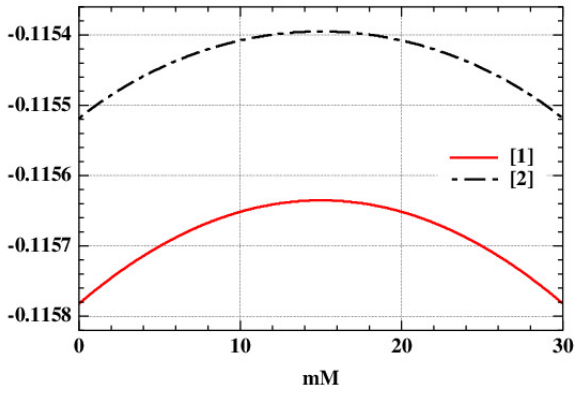

Figure 7: Cross-sections of the Potentials Ψ ($Volts$) for the non-linear boundary condition $\Sigma^s(\Psi)$ with $pH = 7$ in the MSA case: in the middle of the channel [1], at the extremity of the channel [2]. `fig.PB-2coupes-col`

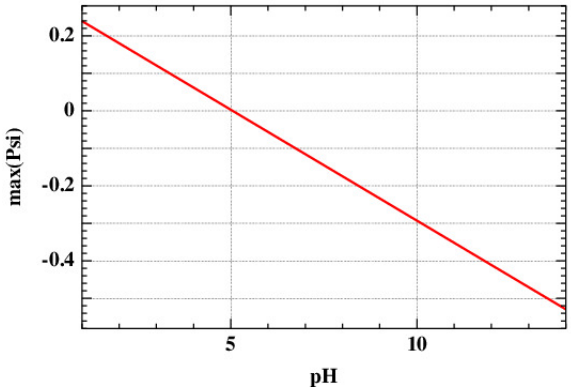

Figure 8: Evolution of the maximum of Ψ (Volts) in Y as a function of the pH in the MSA case. `fig.maxPsi`

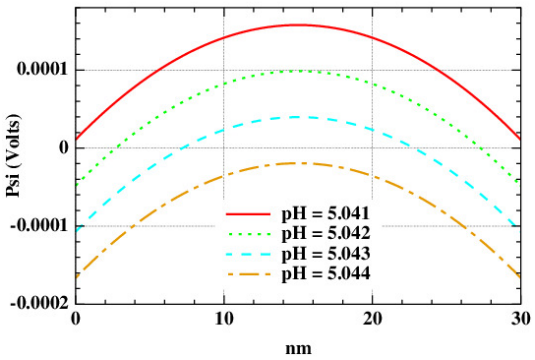

Figure 9: Cross-sections of the potential Ψ in the fluid channel for a single ion H^+ in the MSA case. `fig.poreCrossSection`

ss.multinum

5.4 Numerical results for the multiple ion case

We now consider a $Ca(OH)_2$ salt, meaning that there are 3 different ions, H^+, OH^- and Ca^{2+}, in the electrolyte. All computations are performed for the MSA model. We vary the bulk concentration n_{bulk} of $Ca(OH)_2$ from 10^{-3} to 5.9 10^{-1} mM. From this *reservoir concentration* n_{bulk} we have to deduce the activities a_j of the three ions. In a first step, the activities of the ions Ca^{2+} and OH^- are calculated following the process explained in section 3 of [2]. The main idea to compute these activities is to impose a bulk electroneutrality condition, ensuring that a constant zero surface charge density yields a zero potential. In a second step, knowing the activity a_{OH} of the ion OH^-, the pH of the solution is deduced from the autoprotolysis reaction of water

$$pH = 14 + \log_{10}(a_{OH}),$$

and $a_{OH} = 2\gamma_{OH} n_{bulk}$. Eventually, the H^+ activity is obtained by $a_H = 10^{-pH}$. The H^+ activity is chosen as our characteristic concentration which is used in the adimensionalization process (62). For a concentration $n_{bulk} = 10^{-3}$ mM of $Ca(OH)_2$ the potential Ψ is plotted on Figure 10. The same computation is performed, replacing the non-linear boundary condition $\Sigma^s(\Psi)$ by its constant average Σ^{av}, as defined in (83). The difference between the two resulting potentials is plotted on Figure 11. The largest differences are located at the junctions of the channels, but everywhere the relative difference is of the order of a few percent.

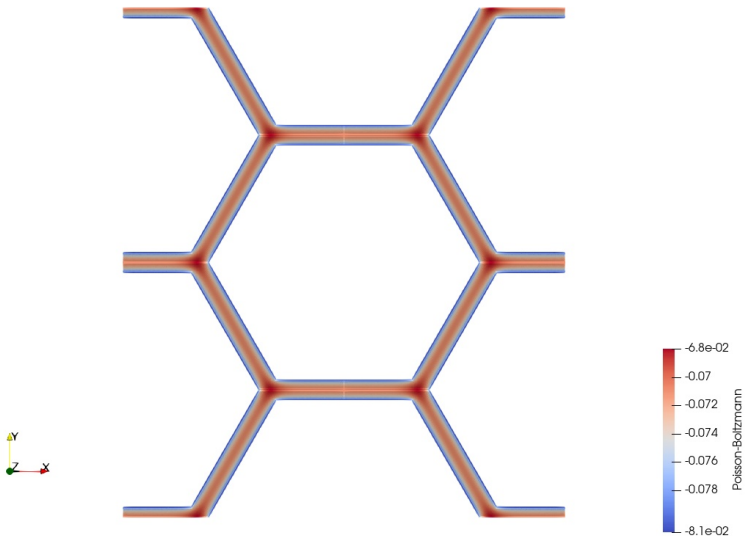

Figure 10: Isovalues of Ψ (Volts) for a concentration $n_{bulk} = 10^{-3}$ mM of $Ca(OH)_2$.

fig.isomulti

Increasing the bulk concentration n_{bulk} we check that the average and the maximum of the surface charge density is monotonically increasing (see Figure 12), while the averaged concentration of the H^+ ion is decreasing (see Figure 13). Of course, in the mean time the averaged concentrations of the OH^- and Ca^{2+} ions are increasing (see Figure 14). From Figure 12 it is obvious that the surface charge is not constant when n_{bulk} varies, which is a clear indication that taking a constant surface charge, as was done in most previous studies, was merely a rough approximation. Let us note that, as in the single ion case, there is a change of sign for the maximum of the potential Ψ:

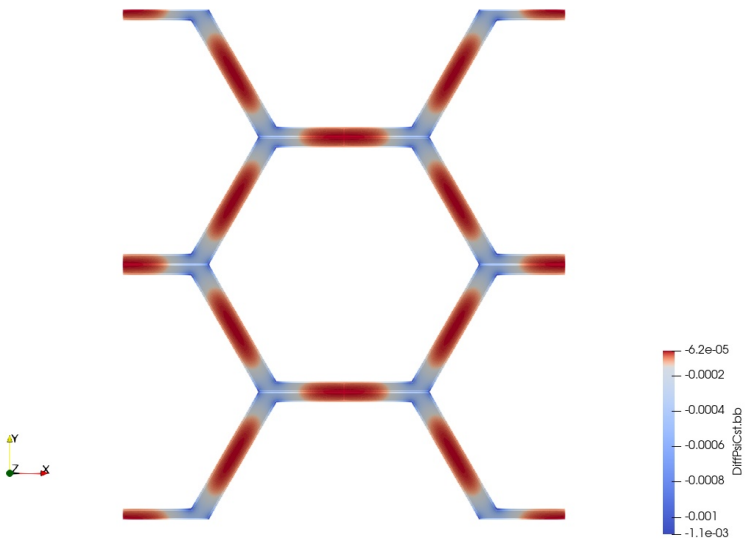

Figure 11: Isovalues of the difference of potential Ψ (Volts) between the non-linear boundary condition $\Sigma^s(\Psi)$ and its constant average Σ^{av} for a concentration $n_{bulk} = 10^{-3}$ mM of $Ca(OH)_2$.

`fig.isomultidiff`

it is positive for low concentrations $n_{bulk} \leq 5.5\ 10^{-7}$ mM and negative for higher concentrations $n_{bulk} \geq 6.\ 10^{-7}$ mM.

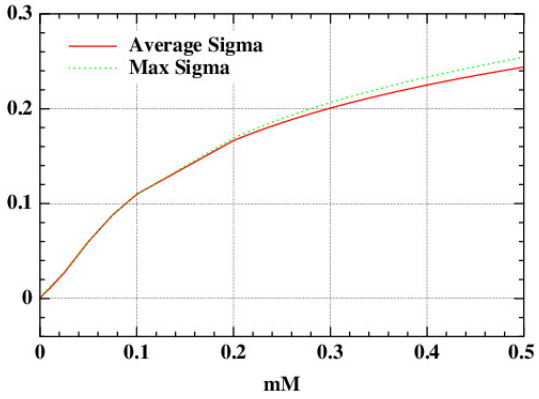

Figure 12: Average and maximum of the surface charge density $\Sigma^s(\Psi)$ as a function of the bulk concentration n_{bulk} of $Ca(OH)_2$.

`fig.SigmaMaxMSA`

As a conclusion, our numerical experiments suggest that the non-linear boundary condition $\Sigma^s(\Psi)$ allows us to find the correct value of the surface charge density which is not the same for all salt reservoir concentrations n_{bulk}. Nevertheless, the relative difference between the resulting potentials is quite small of the order of 1 or 2 percent.

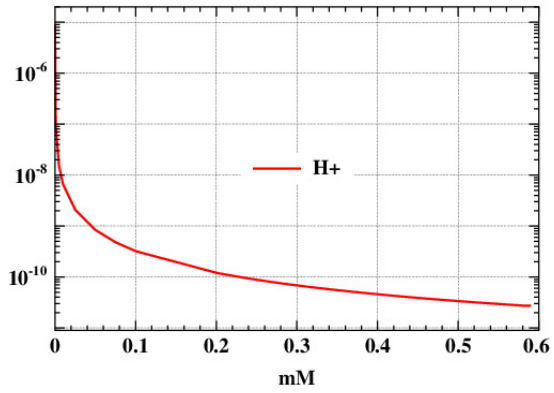

Figure 13: Averaged concentration of H^+ in the pore Y as a function of the bulk concentration n_{bulk} of $Ca(OH)_2$.

fig.averageH+

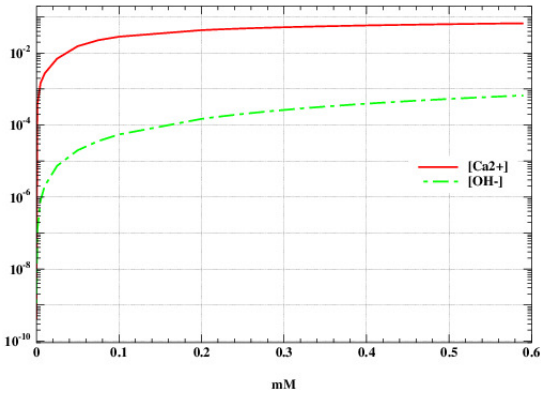

Figure 14: Averaged concentrations of Ca^{2+} and OH^- in the pore Y as a function of the bulk concentration n_{bulk} of $Ca(OH)_2$.

fig.averageOH

References

ABDMP [1] G. Allaire, R. Brizzi, J.-F. Dufrêche, A. Mikelić, A. Piatnitski, *Ion transport in porous media: derivation of the macroscopic equations using upscaling and properties of the effective coefficients,* Comp. Geosci., **17**, Issue 3, 479-495 (2013).

84 [2] G. Allaire, R. Brizzi, J.-F. Dufrêche, A. Mikelic, A. Piatnitski, *Role of non-ideality for the ion transport in porous media: derivation of the macroscopic equations using upscaling,* Physica D, 282, pp.39-60 (2014).

BernardMSA [3] O. Bernard, W. Kunz, P. Turq, L. Blum, *Conductance in Electrolyte Solutions Using the Mean Spherical Approximation*, J. Phys. Chem. **96** (1992), 3833.

Blum77 [4] L. Blum J.S. Hoye: *Mean Spherical Model for Asymmetric Electrolytes. 2. Thermodynamic Properties and the Pair Correlation*, J. Phys. Chem. **81** (1977), 1311.

borkovec [5] M. Borkovec, *Origin of 1-pK and 2-pK models for ionizable water-solid interfaces*, Langmuir 13(10), 2608-2613 (1997).

davis [6] J. A. Davis, R. O. James, J. O. Leckie, *Surface ionization and complexation at the oxide/water interface: I. Computation of electrical double layer properties in simple electrolytes,* Journal of Colloid and Interface Science, 63(3), pp.480-499 (1978).

Dufreche05 [7] J.-F. Dufrêche, O. Bernard, S. Durand-Vidal, P. Turq, *Analytical Theories of Transport in Concentrated Electrolyte Solutions from the MSA*, J. Phys. Chem. B **109** (2005), 9873.

evans [8] L. C. Evans, Partial Differential Equations: Second Edition (Graduate Studies in Mathematics), AMS, Providence, (2010).

FT [9] A. Friedman, K. Tintarev, *Boundary asymptotics for solutions of the Poisson-Boltzmann equation*, J. Differential Equations **69** (1987), 15-38.

Hansen [10] J.-P. Hansen, I. R. McDonald, *Theory of Simple Liquids*, Academic Press, (1986).

freefem [11] F. Hecht. *New development in FreeFem++*, J. Numer. Math., 20(3-4):251–265 (2012).

Hiemstra1996 [12] T. Hiemstra, W. H. Van Riemsdijk, *A Surface Structural Approach to Ion Adsorption: The Charge Distribution (CD) Model*, J. Colloid Interface Sci., 179(2), 488-508 (1996).

KBA:05 [13] G. Karniadakis, A. Beskok, N. Aluru, *Microflows and Nanoflows. Fundamentals and Simulation*, Interdisciplinary Applied Mathematics, Vol. 29, Springer, New York (2005).

L:06 [14] J.R Looker, *Semilinear elliptic Neumann problems and rapid growth in the nonlinearity*, Bull. Austral. Math. Soc., Vol. **74**, no.2, (2006), 161-175.

Pao [15] C. V. Pao, Nonlinear Parabolic and Elliptic Equations, Plenum Press, New York, (1992).

PJ:97 [16] J.-H. Park, J. W. Jerome, *Qualitative properties of steady-state Poisson-Nernst-Planck systems: mathematical study*, SIAM J. Appl. Math. 57 (1997), no. 3, 609-630.

ray [17] N. Ray, A. Muntean, P. Knabner, *Rigorous homogenization of a Stokes-Nernst-Planck-Poisson system,* J. Math. Anal. Appl. 390, no. 1, 374-393 (2012).

schmuck [18] M. Schmuck, M. Z. Bazant, *Homogenization of the Poisson-Nernst-Planck equations for ion transport in charged porous media,* SIAM J. Appl. Math. 75, no. 3, 1369-1401 (2015).

yates [19] D. E. Yates, S. Levine, T. W. Healy, *Site-binding model of the electrical double layer at the oxide/water interface*, J. Chem. Soc., Faraday Trans. 1, 70, pp. 1807-1818 (1974).